JOC The Journal of Organic Chemistry

Article

pubs.acs.org/joc

Structure, Absolute Configuration, and Conformational Study of 12-Membered Macrolides from the Fungus *Dendrodochium* sp. Associated with the Sea Cucumber *Holothuria nobilis* Selenka

Peng Sun,[†,∥] Dong-Xiao Xu,[†,∥] Attila Mándi,[‡] Tibor Kurtán,[‡] Tie-Jun Li,[†] Barbara Schulz,[§] and Wen Zhang*[,†]

[†]Research Center for Marine Drugs and Department of Pharmacology, School of Pharmacy, Second Military Medical University, 325 Guo-He Road, Shanghai 200433, People's Republic of China

[‡]Department of Organic Chemistry, University of Debrecen, POB 20, H-4010 Debrecen, Hungary

[§]Institut für Mikrobiologie, Technische Universität Braunschweig, Spielmannstraße 7, 31806 Braunschweig, Germany

Supporting Information

ABSTRACT: Dendrodolides A–M (**1**–**13**), 13 new 12-membered macrolides, were isolated from *Dendrodochium* sp., a fungus associated with the sea cucumber *Holothuria nobilis* Selenka, which was collected from the South China Sea. The structures of the dendrodolides were elucidated by means of detailed spectroscopic analysis and X-ray single-crystal diffraction. The absolute configurations were assigned using the modified Mosher method, exciton-coupled circular dichroism (ECCD), electronic solution and solid-state circular dichroism (ECD) supported by time-dependent density functional theory (TDDFT) ECD calculations, and X-ray analysis. A detailed conformational analysis of the 13 derivatives indicated that the conformation of the flexible macrolide ring plays a decisive role in their chiroptical properties. Thus, it is highly recommended to apply advanced levels of theory and to avoid simple comparison of ECD spectra to determine the absolute configurations of these derivatives. In an in vitro bioassay, compounds **1**–**5**, **7**–**9**, **11**, and **12** exhibited different levels of growth inhibitory activity against SMMC-7721 and HCT116 cells. This is the first report of 12-membered macrolides from the fungus of the genus *Dendrodochium*. The coisolation of four pairs of epimers is extremely interesting and indicates the complexity of β-ketoreductase stereospecificity in the biosynthesis of enigmatic iterative fungal polyketides.

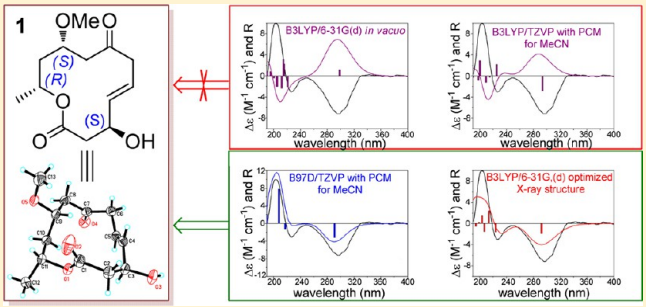

INTRODUCTION

Naturally occurring 12-membered macrolides are a family of fungal hexaketide-derived metabolites that feature a simple 12-membered lactone and an 11-methyl group. Their chemical diversity is attributed to differences in oxidation, e.g., hydroxylation or ketolization at C-3, C-4, C-5, and/or C-7 or double-bond substitution at Δ^2, Δ^4, and/or Δ^8.[1−17] This family of metabolites is relatively rare, and only 19 members have been reported to date. The first example of a 12-membered lactone, recifeiolide, was isolated from the terrestrial fungus *Ceplialosporium recifei* in 1971.[1] Eleven metabolites of such clusters were subsequently isolated from terrestrial fungi, including *C. cladosporioides*,[2,3] *C. tenuissimum*,[8,14] *Ceplialosporium* sp. FT-0012,[10] *Chloridium virescens* var. *Chlamydosporum*,[15] and a *Penicillium urticae* S11R59 mutant.[6,7] Knowledge of this group of metabolites was recently expanded to marine fungi derived molecules upon the discovery of seven macrolides from *Ascomycetous* sp.,[17] the unidentified marine fungus I96S21,[9] *C. herbarum*,[11] and two species of the genus *Ceplialosporium* associated with the sponge *Niphates rowi*[13] and alga *Actinotrichia fragilis*,[12] respectively. These metabolites were reported to have phototoxic,[2,3,8] cytotoxic,[12] antifungal,[6,7,10,12] antibacterial,[6,7] and antiviral activities.[17] The flexible ring system and the remarkable bioactivities of these metabolites have attracted great interest as targets for total synthesis.[18−63] In particular, a number of total syntheses of recifeiolide,[24−29] cladospolides,[30−42] and patulolides[43−63] have been reported.

In the course of our ongoing search for biological metabolites from fungi,[64−66] we recently investigated *Dendrodochium* sp., a fungus isolated from the sea cucumber *Holothuria nobilis* Selenka collected from the South China Sea. Previous studies of this species identified two novel linear peptides as inhibitors of HIV-1 integrase, namely integramides A and B.[67] Our investigation of the acetone extract of the solid fermentation of this fungus led to the discovery of 13 new 12-membered macrolides, dendrodolides A–M (**1**–**13**). The structures and absolute configurations of the new compounds were elucidated by means of detailed spectroscopic analysis, X-ray single-crystal

Received: April 22, 2013
Published: June 14, 2013

dx.doi.org/10.1021/jo400861j | J. Org. Chem. 2013, 78, 7030−7047

diffraction, the modified Mosher method, and TDDFT ECD calculations for solution and solid-state conformers. Interestingly, four pairs of epimers were identified, which suggests that the β-ketoreducase stereospecificity of enigmatic iterative fungal PKSs is substantially complex. This is the first report of 12-membered macrolides from the fungus *Dendrodochium* sp. Herein, we report the isolation, structural elucidation, and biological evaluation of these compounds.

RESULTS AND DISCUSSION

The fungus *Dendrodochium* sp. was cultivated on biomalt agar medium for 28 days before extraction with acetone. The crude extract was fractionated by column chromatography on silica gel and Sephadex LH-20 followed by RP-HPLC to yield pure dendrodolides A–M (**1**–**13**).

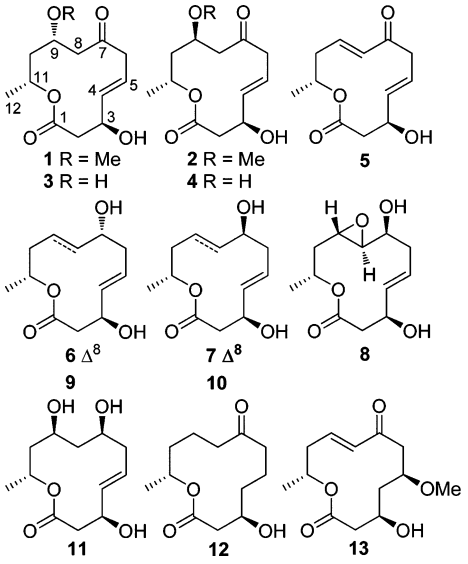

Dendrodolide A (**1**) was obtained as optically active, colorless crystals. Its molecular formula $C_{13}H_{20}O_5$ was established by HRESIMS, which indicated four double-bond equivalents in the molecule. The IR spectrum of **1** displayed absorptions for hydroxy (3420 cm^{-1}) and ester (1723 cm^{-1}) groups. This observation was in agreement with signals in the ^{13}C NMR and DEPT spectra (Tables 1 and 2) for 4 sp^2 carbon atoms (1 × OC═O, 1 × C═O, 1 × CH═CH) at low field and 9 sp^3 carbon atoms at high field (4 × CH_2, 1 × CH_3, 3 × OCH, 1 × OCH_3), accounting for three double-bond equivalents. The remaining double-bond equivalent is due to the presence of one ring in the molecule. The HSQC spectrum facilitated the assignment of the protons to the corresponding carbon atoms. Analysis of the $^1H-^1H$ COSY data revealed two isolated spin systems, i.e., H_2-2 to H_2-6 and H_2-8 to H_3-12. The connection between the two spin systems was elucidated from the observation of HMBC correlations from H_2-6 and H_2-8 to C-7 and from H_2-2 and H-11 to C-1, which lead to the formation of a 12-membered lactone ring (Figure 1). A C-9 methoxy substituent was supported by the HMBC correlation from OMe to C-9.

The *E* geometry of the Δ^4 double bond was assigned based on the large coupling constant of $^3J_{H4,H5}$ (J = 15.0 Hz, in pyridine-d_5) (Table S1 in the Supporting Information). The NOE cross peaks of H-8β with H-4 and H-9 and of H-9 with H-11 indicated a β configuration of these protons, whereas the distinct NOE effect between H-5 and H-3 suggested that these protons have an α orientation (Figure 2).

Table 1. ^1H NMR Spectroscopic Data for Dendrodolides A–D (1–4)[a]

no.	1	2	3	4
2α	2.74 (dd, 14.0, 4.0)	2.63 (dd, 13.5, 2.3)	2.73 (dd, 14.0, 6.0)	2.59 (dd, 13.5, 3.0)
2β	2.62 (dd, 14.0, 7.2)	2.76 (dd, 13.5, 4.6)	2.67 (dd, 14.0, 3.5)	2.76 (dd, 13.5, 5.0)
3	4.56 (br s)	4.61 (br s)	4.59 (br s)	4.58 (m)
4	5.73 (ov)	5.80 (m)	5.79 (dd, 15.5, 4.0)	5.74 (d, 15.0)
5	5.73 (ov)	5.78 (m)	5.71 (m)	5.83 (m)
6α	3.09 (dd, 14.0, 4.0)	3.20 (dd, 15.0, 9.0)	3.10 (dd, 12.5, 7.5)	3.20 (dd, 15.5, 8.5)
6β	3.25 (dd, 14.0, 7.0)	3.08 (dd, 15.0, 2.5)	3.16 (dd, 12.5, 6.0)	3.10 (dd, 15.5, 5.5)
8α	2.46 (dd, 13.0, 8.5)	2.27 (dd, 14.0, 10.0)	2.40 (dd, 15.0, 7.50	2.10 (dd, 14.0, 10.5)
8β	2.87 (dd, 13.0, 5.5)	2.73 (dd, 14.0, 4.0)	2.94 (dd, 15.0, 4.0)	2.90 (dd, 14.0, 2.0)
9	3.65 (m)	3.93 (m)	3.92 (m)	4.16 (m)
10α	1.59 (m)	2.07 (ddd, 14.0, 11.0, 4.0)	1.72 (m)	2.05 (ddd, 14.0, 11.0, 3.0)
10β	1.59 (m)	1.49 (ddd, 14.0, 10.0, 3.0)	1.72 (m)	1.59 (ddd, 14.0, 10.5, 3.5)
11	5.27 (m)	5.05 (m)	5.25 (m)	5.05 (m)
12	1.24 (d, 6.40	1.28 (d, 6.0)	1.23 (d, 6.5)	1.29 (d, 6.5)
OMe	3.37 (s)	3.33 (s)		

[a]In $CDCl_3$; assignments made by DEPT, $^1H-^1H$ COSY, HMQC, HMBC, and NOESY experiments. Values are given in ppm, with multiplicities and coupling constants (in Hz) given in parentheses.

The structure and relative configuration of **1** were further confirmed by a single-crystal X-ray diffraction analysis. The X-ray diffraction analysis also established the absolute configuration of **1** as 3*S*,9*S*,11*R* (Figure 3) with a convincing absolute structure parameter of −0.1(2).[68]

To investigate the solution conformers of **1** and test the applicability of the TDDFT ECD calculation for the determination of absolute configuration, a conformational analysis was performed. The initial MMFF conformational search of (3*S*,9*S*,11*R*)-**1** resulted in 91 conformers in a 21 kJ/mol energy window, indicating high flexibility of the macrolide ring. The B3LYP/6-31G(d) optimization of these conformers in vacuo yielded 10 conformers above 1% (Figure S1 in the Supporting Information). ECD calculations were performed with these conformers and various functionals and the TZVP basis set. In contrast to our expectation, the Boltzmann-averaged ECD spectra were nearly the mirror image of the experimental ECD curve (Figure 4a for the PBE0/TZVP ECD spectrum), possibly because the lowest-energy B3LYP/6-31G(d) conformer in vacuo (Figure 5a) was different from that observed in the X-ray analysis. Therefore, all 91 MMFF conformers were reoptimized at the B3LYP/TZVP level with the PCM solvent model for MeCN.[64,69,70] The larger basis set and the solvent model afforded 12 conformers above 1% (Figure S2 in the Supporting Information), and the lowest-energy conformer (Figure 5b) was different from that obtained by the previous method. Although the ECD spectra of the lowest-energy conformer were similar to the experimental spectra at the three levels applied (B3LYP/TZVP, BH&HLYP/TZVP and PBE0 with PCM for MeCN), the Boltzmann-averaged ECD spectra were still nearly mirror images of the measured spectra (Figure 4b). Therefore, all of the MMFF

dx.doi.org/10.1021/jo400861j | J. Org. Chem. 2013, 78, 7030–7047

Table 2. ^{13}C NMR Spectroscopic Data for Dendrodolides A–H (1–8)[a]

no.	1	2	3	4	5	6	7	8
1	170.9 (C)	171.4 (C)	171.5 (C)	171.9 (C)	171.8 (C)	172.4 (C)	172.3 (C)	171.5 (C)
2	41.6 (CH_2)	41.3 (CH_2)	41.5 (CH_2)	41.2 (CH_2)	41.1 (CH_2)	40.5 (CH_2)	40.7 (CH_2)	40.8 (CH_2)
3	68.6, CH	67.4 (CH)	68.1 (CH)	67.6 (CH)	67.9 (CH)	67.6 (CH)	67.8 (CH)	67.3 (CH)
4	136.8 (CH)	137.2 (CH)	138.3 (CH)	137.3 (CH)	136.2 (CH)	134.7 (CH)	135.4 (CH)	134.1 (CH)
5	124.5 (CH)	122.8 (CH)	123.1 (CH)	122.5 (CH)	124.1 (CH)	125.1 (CH)	123.8 (CH)	123.7 (CH)
6	47.3 (CH_2)	46.2 (CH_2)	48.6 (CH_2)	46.2 (CH_2)	44.9 (CH_2)	40.4 (CH_2)	38.7 (CH_2)	35.7 (CH_2)
7	206.1 (C)	207.5 (C)	209.5 (C)	209.5 (C)	199.3 (C)	73.7 (CH)	70.4 (CH)	66.8 (CH)
8	49.1 (CH_2)	46.3 (CH_2)	47.4 (CH_2)	46.8 (CH_2)	132.4 (CH)	135.3 (CH)	135.1 (CH)	63.1 (CH)
9	74.8 (CH)	73.7 (CH)	67.3 (CH)	65.6 (CH)	144.0 (CH)	130.2 (CH)	124.9 (CH)	53.0 (CH)
10	41.0 (CH_2)	37.7 (CH_2)	43.1 (CH_2)	42.3 (CH_2)	38.9 (CH_2)	40.9 (CH_2)	40.6 (CH_2)	38.9 (CH_2)
11	69.4 (CH)	68.1 (CH)	70.3 (CH)	68.4 (CH)	69.9 (CH)	69.2 (CH)	69.6 (CH)	68.6 (CH)
12	20.9 (CH_3)	20.9 (CH_3)	21.2 (CH_3)	20.7 (CH_3)	20.9 (CH_3)	20.9 (CH_3)	20.8 (CH_3)	21.2 (CH_3)
OMe	56.9 (CH_3)	55.8 (CH_3)						

[a]In $CDCl_3$; assignments made by DEPT, $^1H–^1H$ COSY, HMQC, HMBC, and NOESY experiments. Values are given in ppm, with assignments given in parentheses.

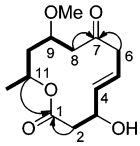

Figure 1. $^1H–^1H$ COSY (bold) and selected HMBC (arrow) correlations of **1**.

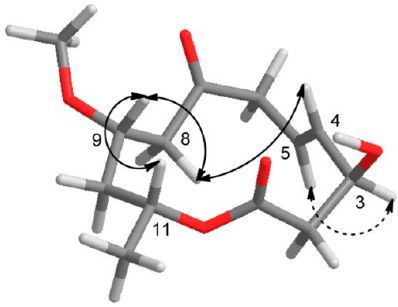

Figure 2. Key NOE correlations of **1**.

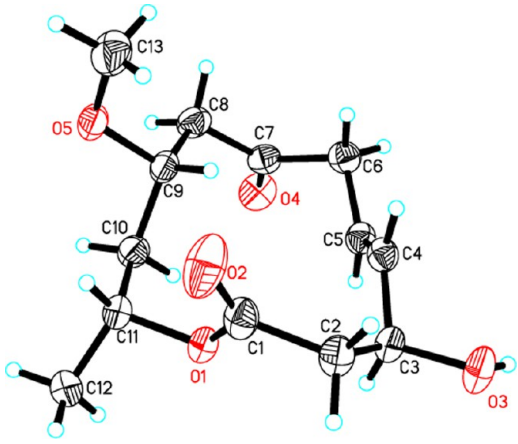

Figure 3. Single-crystal X-ray structure of **1** (ORTEP drawing).

conformers were reoptimized at the more advanced B97D/TZVP level[71] with the PCM model for MeCN, resulting in 14 conformers above 1% (Figure S3 in the Supporting Information). In this case, the Boltzmann-weighted average ECD spectra were in good agreement with the measured spectra (Figure 4c), although the lowest energy conformer (Figure 5c) was similar to that of the B3LYP/TZVP method and that of the solid-state X-ray conformer (Figure 5d).

The computed conformers of **1** can be sorted into two groups (Figure 5) depending on the orientation of the Δ^4 double bond. When oriented as in Figure 5, H-4 is pointing upward in the low-energy conformers and downward in the high-energy conformers. The two types of conformers have nearly mirror-image ECD spectra, and hence the accurate estimation of their Boltzmann population is critical for the correct assignment of the absolute configuration. The widely applied B3LYP functional failed to predict the population of the solution conformers properly for this derivative, and the B97D functional is required to treat the conformers of this flexible macrolide appropriately. Because the structure of the solid-state conformer was available from the X-ray analysis, ECD was also calculated for the DFT optimized solid-state conformer (Figure 5d), which gave fairly good agreement with the experimental solution ECD spectrum (Figure 4d). Unfortunately, our attempts to prepare KCl pellets of acceptable quality for solid-state ECD measurements failed and thus the solid-state ECD protocol[72] could not be applied. However, it is evident from the solution ECD spectrum that the solid-state conformer must be represented by a large population in solution as well.

Dendrodolide B (**2**), the major metabolite of the fungus, was isolated as an optically active, colorless oil. Its molecular formula was the same as that of **1**, as established by HRESIMS. The NMR data of **2** (Tables 1 and 2) were similar to those of **1**, with the exception of the ^{13}C NMR values for C-8, C-9, and C-10 (δ_C 46.3, 73.7, and 37.7 in **2**; δ_C 49.1, 74.8, and 41.0 in **1**), suggesting a different configuration of OH-9. The observed NOE effect between H-9 and H-11 in **1** was absent in **2** (Figure 6). Instead, distinct NOE correlations of H-8β with H-11 and H-5 and of H-6α with H-9 and H-4 were observed, supporting the above assignment of H-9 as the α orientation. Thus, the relative configuration of **2** was determined as 3*S**,9*R**,11*R**.

The 3*S* absolute configuration of **2** was determined using the modified Mosher method by measuring the differences in the chemical shifts of the (*R*)-MPA ester at different temperatures (Figure 7).[73] The same conclusion could be drawn by using the exciton-coupled CD (ECCD) method[74] on the 3-(*p*-methoxybenzoate) derivative (Figure 8). According to the allylic benzoate method, if the exciton coupling between the double bond and the benzoate group produces a positive band (λ 259

dx.doi.org/10.1021/jo400861j | J. Org. Chem. 2013, 78, 7030–7047

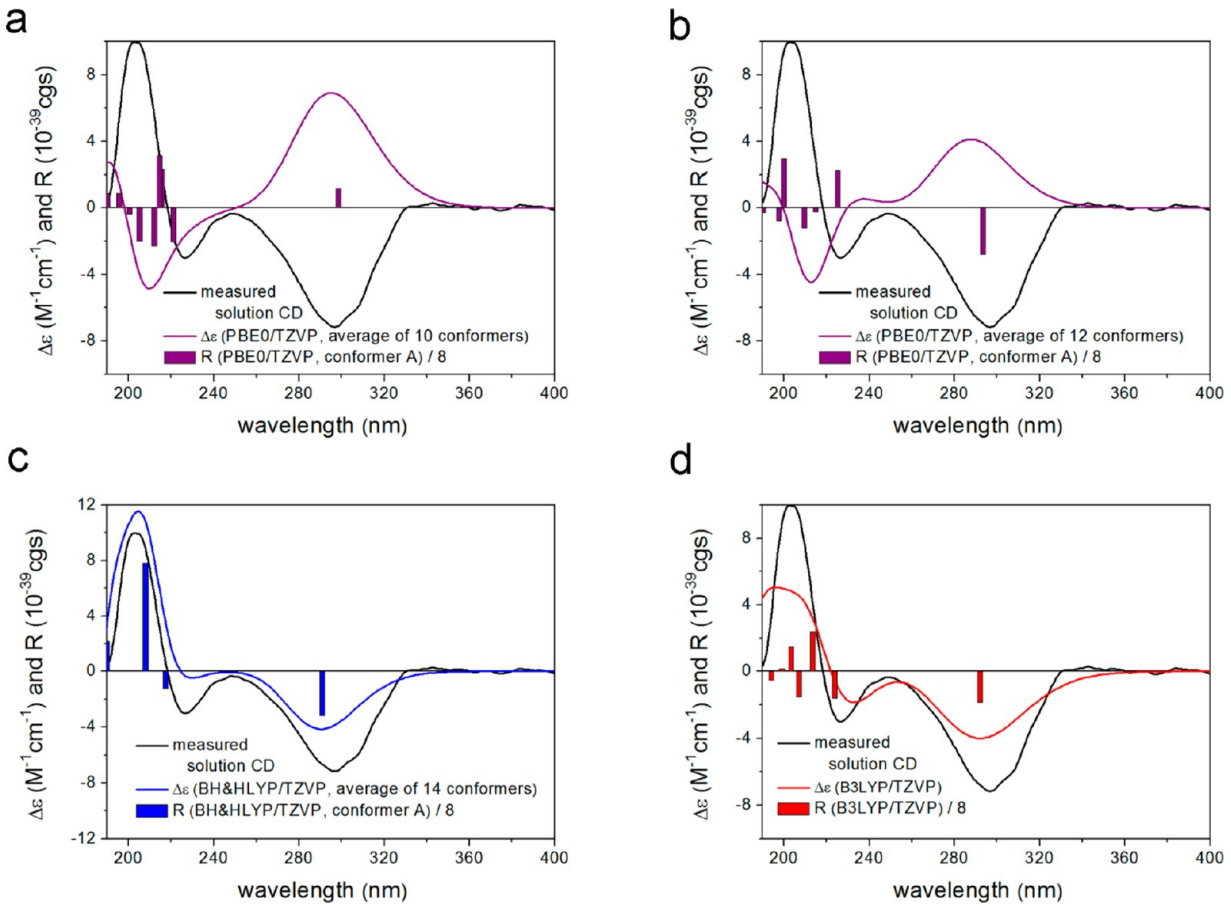

Figure 4. Experimental and Boltzmann-averaged ECD spectra of (a) B3LYP/6-31G(d) conformers at the PBE0/TZVP level in vacuo, (b) B3LYP/TZVP with PCM for MeCN conformers at the PBE0/TZVP level with PCM for MeCN, (c) B97D/TZVP with PCM for MeCN conformers at the BH&HLYP/TZVP level with PCM for MeCN, and (d) B3LYP/6-31G X-ray structure at B3LYP/TZVP in vacuo of **1**. Bars represent rotational strength values of the lowest energy conformers at each level.

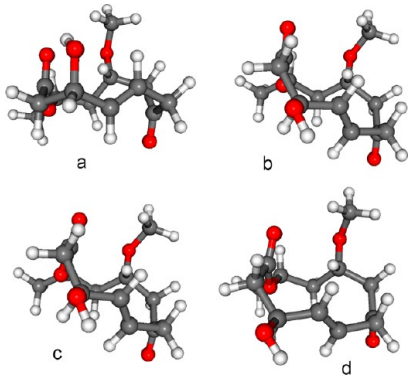

Figure 5. Structure of the lowest energy conformer of **1** obtained at (a) B3LYP/6-31G(d) level in vacuo, (b) B3LYP/TZVP level with PCM for acetonitrile, (c) B97D/TZVP with PCM for acetonitrile, and (d) B3LYP/6-31G(d) optimized X-ray structure.

nm, $\Delta\varepsilon$ = +1.52), the electric transition moments of the two interacting chromophores have positive chirality with an *S* absolute configuration of the original alcohol.

Dendrodolide B (**2**) is the C-9 epimer of **1**, and its ECD spectra exhibited opposite Cotton effects (CEs) for the n−π* (296 nm) and π−π* (203 nm) transitions (Figure 9). To determine the origin of their near mirror-image ECD spectra, conformational analysis and TDDFT ECD calculations were performed.

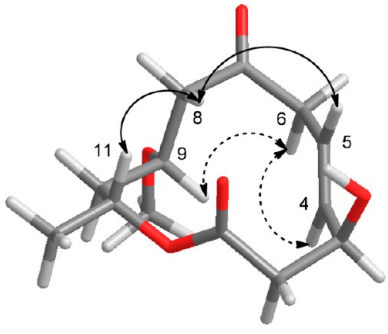

Figure 6. Key NOE correlations of **2**.

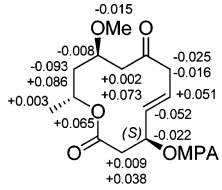

Figure 7. $\Delta\delta^{T1T2}$ ($\delta^{T1} - \delta^{T2}$, T1 = 25 °C, T2 = −25 °C) values (in ppm) for the (*R*)-MPA ester of **2**.

The MMFF conformational search of **2** resulted in 112 conformers, which were reoptimized at the levels B3LYP/6-31G(d) in vacuo, B3LYP/TZVP with PCM for MeCN, and

dx.doi.org/10.1021/jo400861j | J. Org. Chem. 2013, 78, 7030−7047

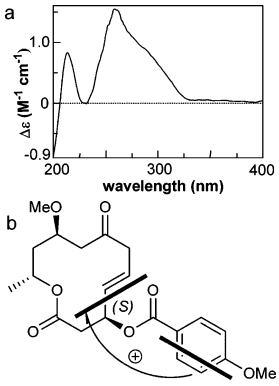

Figure 8. ECD spectrum (a) and structure (b) of **2**-*p*-methoxybenzoate.

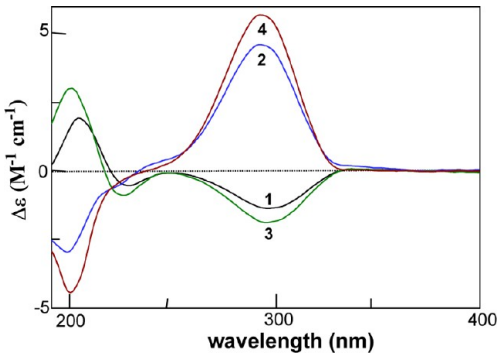

Figure 9. Solution ECD spectra of dendrodolides A–D (**1**–**4**).

B97D/TZVP with PCM for MeCN, yielding 10, 5, and 5 conformers above 1%, respectively. The B97D/TZVP conformers with PCM for MeCN are presented in Figure 10, which shows that 3-OH has an axial orientation, in accordance with the small $^{3}J_{H2,H3}$ coupling constant values (Table 1). In the low-energy conformers, the 3-OH is hydrogen-bonded to the oxygen of the lactone carbonyl group, and the conformation of the macrolide ring resembles the minor conformers of **1**.

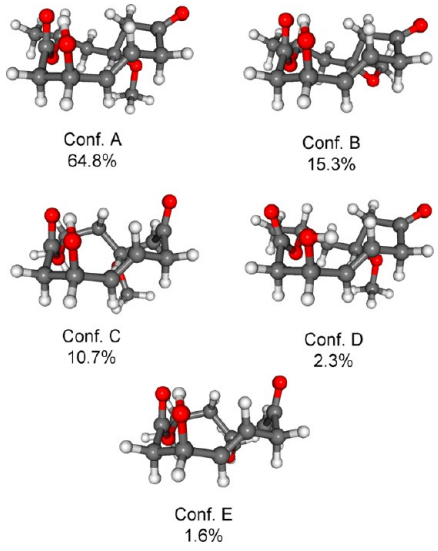

Figure 10. Low-energy conformers (≥1%) of **2** obtained by optimization with B97D/TZVP with PCM for MeCN.

TDDFT ECD calculations were performed with three methods for the low-energy conformers obtained at the three levels of conformational analysis. The ECD spectra calculated for the B3LYP/6-31G(d) in vacuo optimized conformers were in fairly good agreement with the experimental spectrum (Figure 11), while those calculated for the solvent model-

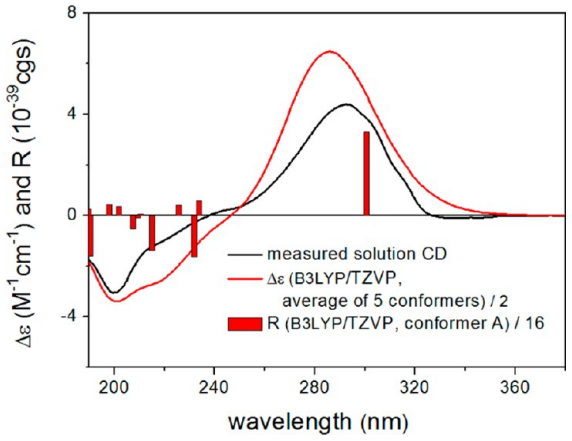

Figure 11. Experimental and Boltzmann-averaged ECD spectra of **2** (optimization level B97D/TZVP with PCM for MeCN, ECD level B3LYP/TZVP with PCM for MeCN). Bars represent rotational strength values of the lowest energy conformer.

optimized conformers improved it further, allowing the unambiguous determination of the absolute configuration as 3*S*,9*R*,11*R*. The inversion of the C-9 chirality center in **2** apparently changed the preferred conformation of the macrolide ring, which was responsible for the opposite CEs in comparison to those of **1**.

Dendrodolide C (**3**) was obtained as an optically active, colorless oil. The ^{1}H and ^{13}C NMR spectra of **3** (Tables 1 and 2) were almost identical with those of **1**, with the exception of the disappearance of the signals for the methoxy group (δ_C 56.9, δ_H 3.37). This conclusion is in agreement with the molecular formula of $C_{12}H_{18}O_5$ deduced by HRESIMS, which showed that **3** had 14 fewer mass units than **1**. The obvious upfield-shifted value of C-9 (δ_C 74.8 in **1** and 67.3 in **3**) supports that **3** is the 9-demethyl derivative of **1**. The proposed structure was further confirmed by the proton sequence from H_2-8 to H_3-12 established by an ^{1}H–^{1}H COSY experiment. The relative configuration of **3** was confirmed to be the same as that of **1** by NOESY analysis. The absolute configuration of **3** was consequently determined as 3*S*,9*S*,11*R* due to the congruent ECD curves of **1** and **3** (Figure 9). The B3LYP/6-31G(d) in vacuo and B97D/TZVP PCM/MeCN reoptimizations of the 114 MMFF conformers of **3** yielded 4 and 14 (Figure 12 and Figure S4 (Supporting Information)) conformers above 1%, respectively. Similar to the case for **1**, the ECD spectra calculated for the B3LYP/6-31G(d) in vacuo conformers of **3** were nearly the mirror image of the experimental spectrum. The higher basis set, solvent model, and advanced functional applied for the reoptimizations improved the agreement, although in contrast to **1**, this reoptimization was not sufficient to reproduce all the ECD transitions correctly. All three methods applied to the ECD calculations for the B97D/TZVP PCM/MeCN conformers reproduced well the two high-energy transitions at approximately 223 and 197 nm, but the negative 295 nm transition could not be predicted well (Figure 13). This discrepancy is

dx.doi.org/10.1021/jo400861j | J. Org. Chem. 2013, 78, 7030–7047

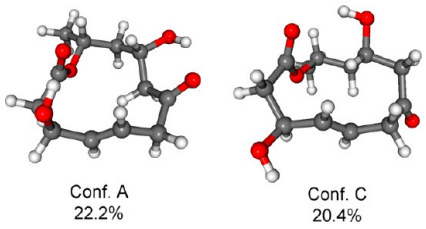

Figure 12. B97D/TZVP PCM/MeCN reoptimized low-energy conformers of **3** representing the two types of macrolide conformations.

most likely due to the underestimation of the population of conformers represented by conformer C.

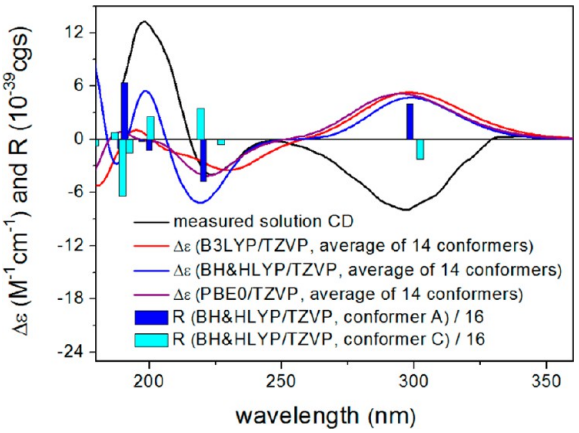

Figure 13. Experimental and Boltzmann-averaged ECD spectra of **3** (optimization level B97D/TZVP with PCM for MeCN). Bars represent rotational strength values of conformers A (lowest-energy type A conformer, blue) and C (lowest-energy type B conformer, light cyan).

Dendrodolide D (**4**), a colorless crystal, has a molecular formula of $C_{12}H_{18}O_5$, as established by HRESIMS. The ^1H and ^{13}C NMR spectroscopic data for **4** (Tables 1 and 2) are very similar to those for **2**. Similar to the case for **3** vs **1**, the signals for the methoxy group (δ_C 55.8, δ_H 3.33) in **2** were absent in **4**, suggesting that **4** is the 9-demethyl derivative of **2**. The proposed structure was strongly supported by 2D NMR experiments. Compound **4** exhibited the same ECD pattern as **2**, suggesting that the two compounds are homochiral, which allowed the determination of its absolute configuration as 3*S*,9*R*,11*R* on the basis of the established relative configuration. The MMFF conformational search produced 121 conformers, which were reoptimized at the levels B3LYP/6-31G(d) in vacuo, B3LYP/TZVP with PCM for MeCN, and B97D/TZVP with PCM model for MeCN to yield 4, 8, and 7 (Figure 14) conformers above 1%, respectively. Although the intensities of the ECD spectra calculated for the B3LYP/6-31G(d) in vacuo optimized conformers were much weaker than those of either the solvent model spectrum or the experimental spectrum (Figure 15), all applied levels allowed unambiguous determination of the absolute configuration as 3*S*,9*R*,11*R*. The solid-state ECD spectrum of **4** could be recorded as a KCl pellet and was nearly identical with the solution spectrum. The ECD spectra calculated for the optimized X-ray conformer were in good agreement with the solid-state and solution experimental and Boltzmann-weighted calculated spectra. This agreement proved that the conformers represented by the X-ray geometry

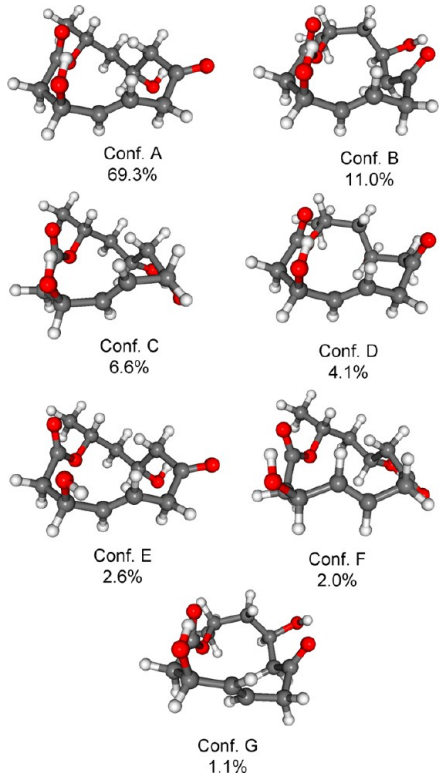

Figure 14. B97D/TZVP with PCM for MeCN reoptimized low-energy conformers (≥1%) of **4**.

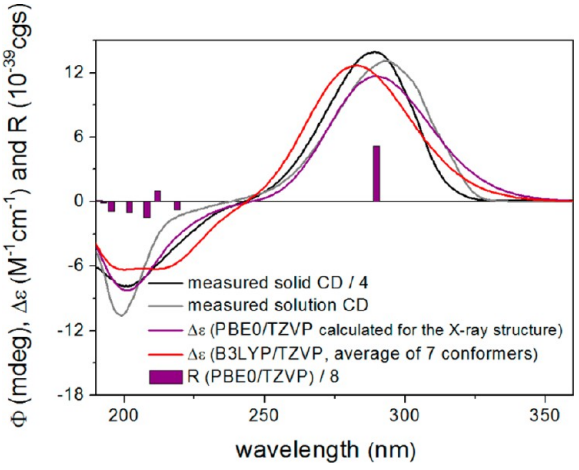

Figure 15. Experimental solid-state and solution spectra, PBE0/TZVP spectrum calculated for the optimized X-ray structure, and Boltzmann-averaged spectrum of **4** (optimization level B97D/TZVP with PCM for MeCN, ECD level B3LYP/TZVP with PCM for MeCN). Bars represent rotational strength values of the X-ray conformer.

are also dominant in solution and that they are responsible for the observed ECD transitions in the solution and solid-state spectra. The absolute configuration of **4** was further confirmed by single-crystal X-ray diffraction (Figure 16) with an absolute structure parameter of −0.2(3).

Dendrodolide E (**5**) was isolated as an optically active colorless oil with the molecular formula $C_{12}H_{16}O_4$, as deduced by HRESIMS, which revealed that **5** had 18 fewer mass units than **4**. The ^{13}C spectrum of **5** (Table 2) resembled that of **4**, with the exception that an oxygenated methine (δ_C 65.6) and methylene (δ_C 46.8) in **4** were replaced by a pair of double

dx.doi.org/10.1021/jo400861j | J. Org. Chem. 2013, 78, 7030−7047

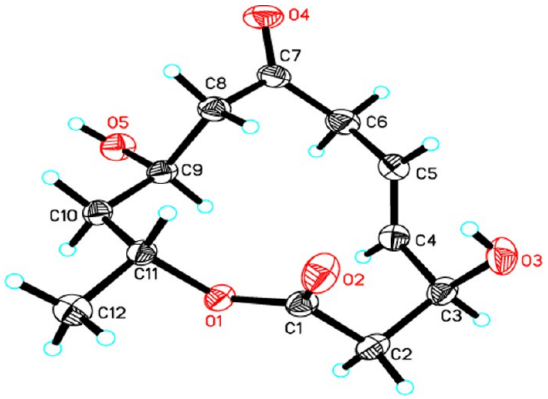

Figure 16. Single-crystal X-ray structure of **4** (ORTEP drawing).

bonds (δ_C 132.4 and 144.0) in **5**. The assignment of the double bond as Δ^8 was confirmed by the proton sequence from H-8 to H_3-12 established by a $^1H-^1H$ COSY experiment. The *E* geometry of Δ^8 was deduced from the large coupling constant between the olefinic protons ($^3J_{H8,H9}$ = 16.5 Hz). The relative configuration of all of the other asymmetric centers remained intact on the basis of the NOESY experiment.

The MMFF conformational search resulted in 51 conformers for **5**, which were reoptimized at the B3LYP/6-31G(d) in vacuo and B97D/TZVP with PCM model for MeCN levels, yielding 5 and 6 (Figure 17) conformers above 1%, respectively. The

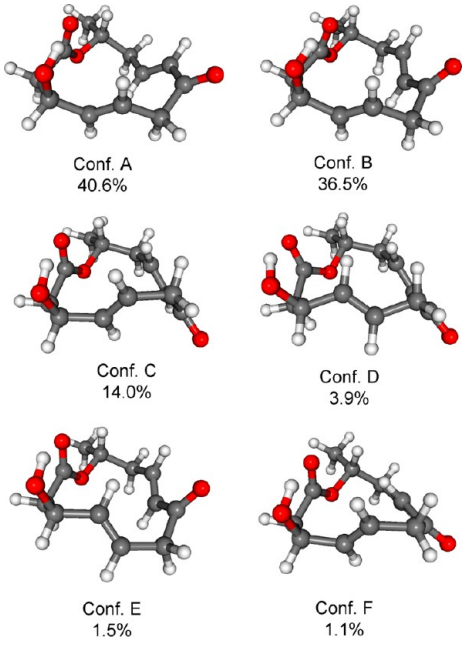

Figure 17. B97D/TZVP with PCM for MeCN reoptimized low-energy conformers (≥1%) of **5**.

ECD calculations were in good agreement for the conformers optimized at both levels; however, B97D with a larger basis set and solvent model achieved slightly better results. The conformation of the α,β-unsaturated enone chromophore is crucial for the calculation of the ECD spectrum. The 3-OH was hydrogen-bonded to the oxygen of the lactone carbonyl in all conformers, while the relative arrangement of the ketone carbonyl and the two double bonds varied. The B97D/TZVP method computed the lowest energy conformer A with 40.6% population; the same conformer was identified by B3LYP/6-31G(d) as the second lowest energy conformer with 25.5% population. Because the ECD spectrum of conformer A was very similar to the experimental spectrum, its higher population in the B97D/TZVP method improved the agreement between the computed and experimental curves (Figure 18). The good

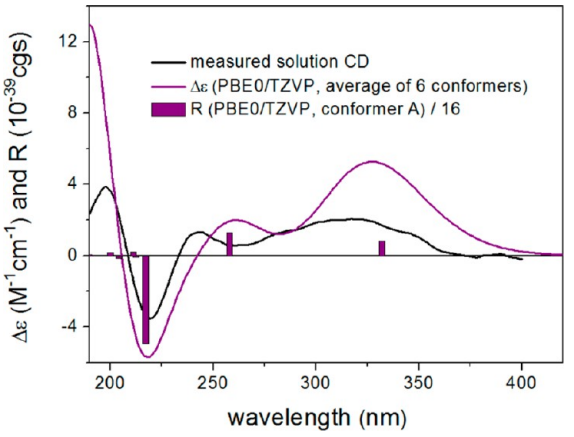

Figure 18. Experimental and Boltzmann-averaged ECD spectra of **5** (optimization level B97D/TZVP with PCM for MeCN, ECD level PBE0/TZVP with PCM for MeCN). Bars represent rotational strength values of the lowest energy conformer.

agreement allowed the unambiguous assignment of the absolute configuration as 3*S*,11*R*. Thus, **5** is determined as the C-3 epimer of balticolid isolated previously from the marine fungus *Ascomycetous* sp.[17]

Dendrodolide F (**6**), an optically active, colorless oil, has a molecular formula of $C_{12}H_{18}O_4$, as deduced by HRESIMS. Comparison of the overall ^{13}C and ^1H NMR spectroscopic data for **6** (Tables 2 and 3) revealed great similarity with those of **5**. However, the C-7 keto group of **5** is replaced by a hydroxy group (δ_C 73.7, δ_H 4.05) in **6**, as confirmed by the proton connection from H_2-2 to H_3-12 deduced by $^1H-^1H$ COSY. The relative configuration of **6** was assigned by interpretation of the NOESY experiment in pyridine-d_5, in which all of the proton resonance signals were well separated. The β orientation of H-7 was indicated by the distinct NOE effects of H-9 with H-7 and H-11 and of H-7 with H-5, while the α orientation of H-3 was deduced from the NOE cross peak between 3-OH and H-2β observed in the NOESY spectrum (Figure 19). The relative configuration of **6** was then established as 3*S**,7*R**,11*R**, and the absolute configuration was determined by TDDFT ECD calculations of the solution conformers. The MMFF conformational search of **6** resulted in 55 conformers. These conformers were reoptimized at the B3LYP/6-31G(d) in vacuo and B97D/TZVP with PCM model for MeCN levels to yield 2 (Figure 20) and 4 conformers above 1%, respectively. The ECD calculations for the conformers optimized at both levels were in good agreement (Figure 21). The two methods identified the same two conformers as having the lowest energy, explaining the high similarity of the ECD results for this molecule. However, conformer B, which is present at 1.1% and 3.1%, respectively, in the two methods, has nearly mirror-image spectra in comparison to that of conformer A (98.0% and 92.1%, respectively). The nearly exclusive population of conformer A at both levels enabled the safe assignment of the absolute configuration as 3*S*,7*R*,11*R*. The presence of low-energy conformers with nearly mirror-image spectra, however,

dx.doi.org/10.1021/jo400861j | J. Org. Chem. 2013, 78, 7030−7047

Table 3. ^{1}H NMR Spectroscopic Data for Dendrodolides E–H (5–8)[a]

no.	5	6	7	8
2α	2.76 (dd, 14.0, 4.5)	2.45 (dd, 14.0, 2.5)	2.72 (dd, 14.4, 5.4)	2.57 (dd, 13.9, 2.0)
2β	2.51 (dd, 14.0, 2.5)	2.72 (dd, 14.0, 5.2)	2.50 (dd, 14.4, 2.4)	2.75 (dd, 13.9, 5.9)
3	4.53 (s)	4.46 (br s)	4.43 (ov)	4.49 (br s)
4	5.56 (dd, 16.0, 1.0)	5.41 (dd, 15.0, 3.0)	5.43 (m)	5.65 (d, 14.5)
5	5.76 (ddd, 16.0, 6.0, 5.5)	5.53 (ddd, 15.0, 10.5, 4.0)	5.65 (dddd, 15.6, 10.2, 5.4, 1.8)	5.78 (ddd, 14.5, 8.5, 4.0)
6α	3.21 (dd, 14.5, 6.0)	2.09 (ddd, 12.0, 10.5, 8.5)	2.55 (m)	2.35 (dd, 11.5, 11.5)
6β	3.31 (dd, 14.5, 8.0)	2.59 (ddd, 12.0, 4.0, 2.0)	2.21 (m)	2.65 (br d, 11.5)
7		4.05 (ddd, 11.0, 8.5, 4.0)	4.47 (ov)	4.19 (br s)
8α	5.96 (d, 16.5)	5.22 (m)	5.34 (ddd, 15.0, 2.4, 1.8)	2.78 (br s)
9	6.53 (ddd, 16.5, 9.0, 7.0)	5.36 (ddd, 15.0, 11.0, 3.5)	5.44 (ddd, 15.0, 4.2, 1.8)	3.09 (br d, 9.5)
10α	2.28 (ddd, 14.0, 11.0, 9.0)	2.12 (ddd, 14.0, 11.0, 9.5)	2.39 (m)	1.59 (ov)
10β	2.41 (ddd, 14.0, 6.0, 3.0)	2.34 (ddd, 14.0, 4.0, 2.0)	2.17 (m)	2.18 (d, 15.0)
11	5.27 (m)	5.22 (m)	5.23 (m)	5.36 (m)
12	1.32 (d, 6.5)	1.25 (d, 6.6)	1.28 (d, 6.6)	1.26 (d, 6.5)
3-OH		3.90 (d, 10.0)		

[a]In $CDCl_3$; assignments made by DEPT, ^{1}H–^{1}H COSY, HMQC, HMBC, and NOESY experiments. Values are given in ppm, with multiplicities and coupling constants (in Hz) given in parentheses.

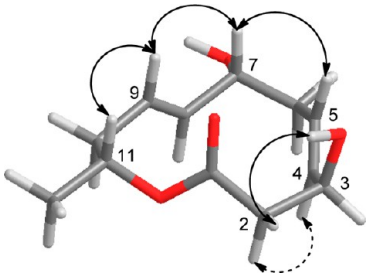

Figure 19. Key NOE correlations of **6**.

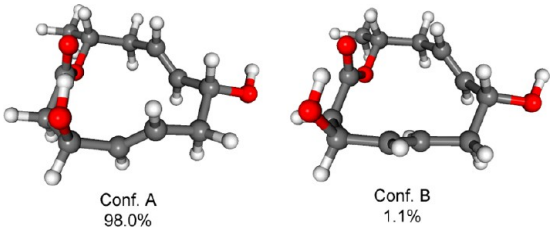

Figure 20. B3LYP/6-31G(d) in vacuo reoptimized low-energy conformers (≥1%) of **6**.

suggests that possible conformations must be thoroughly studied for such a flexible macrolide whenever the absolute configuration is determined by ECD analysis.

The established absolute configurations at C-3 and C-7 were further confirmed by using the modified Mosher method on the secondary hydroxy groups.[73] NMR comparison of the (*R*)- and (*S*)-MPA diesters revealed that all the $\Delta\delta^{R\text{-}S}$ data (Figure 22) were consistent with assignment of **6** as (3*S*,7*R*).

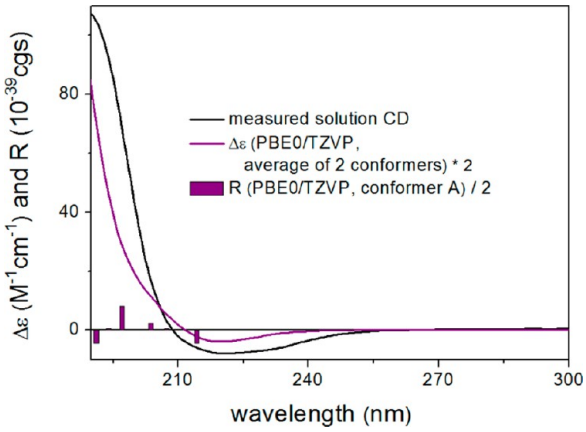

Figure 21. Experimental and Boltzmann-averaged ECD spectra of **6** (optimization level B3LYP/6-31G(d) in vacuo, ECD level PBE0/TZVP in vacuo). Bars represent rotational strength values of the lowest energy conformer.

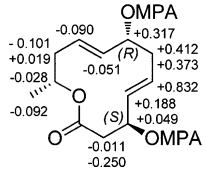

Figure 22. $\Delta\delta^{R\text{-}S}$ values (in ppm) for the MPA diesters of **6**.

Dendrodolide G (**7**) was isolated as an optically active, colorless oil. HRESIMS gave a molecular formula of $C_{12}H_{18}O_4$. The ^{13}C and ^{1}H NMR spectra of **7** (Tables 2 and 3) resembled those of **6**, with the exception of the chemical shift values for C-7 (δ_C 73.7 and δ_H 4.05 in **6**, δ_C 70.4 and δ_H 4.47 in **7**), suggesting a different configuration of 7-OH. The NOESY spectrum of **7** recorded in pyridine-d_5 (Table S1 in the Supporting Information) revealed a different NOE pattern in contrast to that of **6**. The H-5 was oriented in an α configuration, due to the observation of its NOE effect with H-3 (Figure 23). The α configuration of H-7 and H-9 was

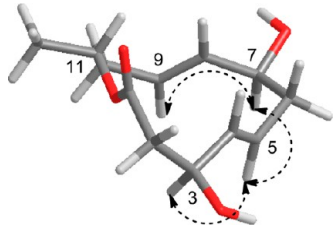

Figure 23. Key NOE correlations of **7**.

consequently determined on the basis of the NOE effect between H-7 and both H-5 and H-9. The assignment is in agreement with the observation that the distinct NOE effect between H-9 and H-11 in **6** is absent in **7**. The relative configuration of **7** was thus established as 3*S**,7*S**,11*R**. The absolute configuration of **7** was determined by TDDFT ECD calculations. The experimental solution ECD was nearly identical with that of **6**, and the B3LYP/6-31G(d) in vacuo and B97D/TZVP PCM/MeCN reoptimizations of the 43 MMFF conformers of **7** (2 (Figure S5, Supporting Information) and 5 conformers above 1%, respectively) gave results similar to those of **6** (Figure S6, Supporting

dx.doi.org/10.1021/jo400861j | J. Org. Chem. 2013, 78, 7030–7047

Information). The computed ECD is mainly dominated by the lowest energy conformer with 88.6% and 64.3% populations. Unlike the case for **6**, the ECD spectrum of conformer B was similar to the ECD spectrum of conformer A down to 206 nm, which makes the results more reliable. Thus, the absolute configuration of **7** was unambiguously determined as 3*S*,7*S*,11*R*.

Dendrodolide H (**8**) was isolated as an optically active, colorless oil with the molecular formula $C_{12}H_{18}O_5$, as determined by HRESIMS. Comparison of the overall ^{13}C and ^1H NMR data (Tables 2 and 3) revealed great similarity of **8** with **7**. However, the signals for Δ^8 of **7** were replaced by those of a typical epoxide functionality (δ_C 63.1 (CH) and 53.0 (CH); δ_H 2.78 (br s) and 3.09 (br d)). The assignment of the epoxide at C-8 and C-9 was supported by the proton sequence from H_2-2 to H_3-12 deduced from the $^1H-^1H$ COSY spectrum. The small $^1H-^1H$ coupling constants between the two epoxide protons ($^3J_{H8,H9} \approx 0$ Hz) indicated a *trans* epoxide unit.[75] The distinct NOE effect of H-11 with H-9 suggested a β orientation for H-9 and, correspondingly, an α orientation for H-8. The relative configuration of the rest of the chiral centers was same as that of **7** on the basis of the NOESY experiment (Figure S7, Supporting Information), leading to the assignment of the relative configuration of **8** as 3*S**,7*S**,8*S**,9*S**,11*R**. A positive CE that appeared at 219 nm in the solution ECD of **8** was different from those of all other dendrodolides and is most likely due to conformational changes caused by the epoxide moiety. The B3LYP/6-31G(d) in vacuo and B97D/TZVP PCM/MeCN reoptimizations (resulting in 3 (Figure 24) and 7

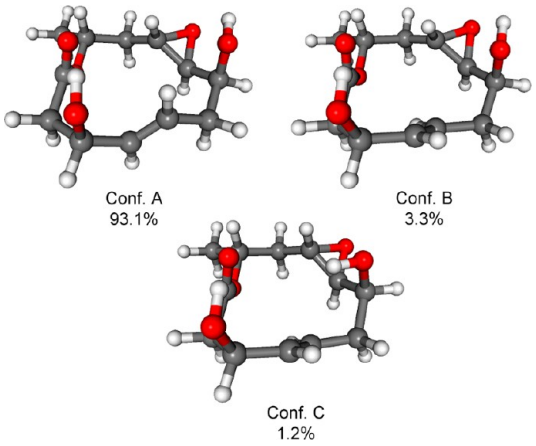

Figure 24. B3LYP/6-31G(d) in vacuo reoptimized low-energy conformers (≥1%) of **8**.

conformers above 1%, respectively) of the 38 MMFF conformers of (3*S*,7*S*,8*S*,9*S*,11*R*)-**8** support this assumption. The preferred conformation of the macrolide ring is governed by the hydrogen bonding of the two hydroxyl groups. The ECD calculations performed on the low-energy conformers revealed that the observed ECD is an average of two types of conformers. However, similar to the case for **7**, the ECD spectra of the two types of conformers do not cancel each other. All three levels applied for the ECD calculations (B3LYP/TZVP, BH&HLYP/TZVP and PBE/TZVP, all with PCM for MeCN) of the B97D/TZVP PCM/MeCN conformers gave fairly good agreement with the experimental ECD spectra (Figure 25). This is also true for the B3LYP/TZVP and PBE0/TZVP in vacuo Boltzmann-averaged ECD spectra computed for the B3LYP/6-31G(d) gas-phase conformers,

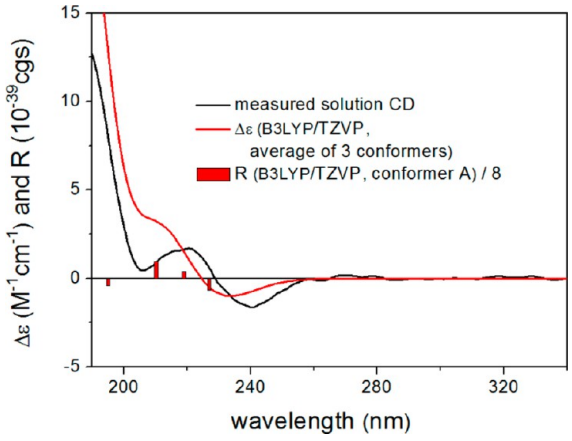

Figure 25. Experimental and Boltzmann-averaged ECD spectra of **8** (optimization level B3LYP/6-31G(d) in vacuo, ECD level B3LYP/TZVP in vacuo). Bars represent rotational strength values of the lowest energy conformer.

with B3LYP/TZVP giving the best agreement. The BH&HLYP in vacuo ECD calculation computed for the B3LYP/6-31G(d) gas-phase conformers did not match the experimental ECD curve (there may be notable deviations from the estimated Boltzmann weights[76]). Notably, this BH&HLYP method gave good results in most of the above derivatives. The agreement of the ECD calculations with the other five methods as well as biosynthetic considerations[77] allowed the assignment of the absolute configuration of **8** as 3*S*,7*S*,8*S*,9*S*,11*R*.

Dendrodolide I (**9**) was obtained as colorless crystals. The ^1H and ^{13}C NMR spectra of **9** (Tables 4 and 5) were highly similar to those of **6**, with the exception of the absence of the signals for the Δ^8 double bond. This is in agreement with the molecular formula of $C_{12}H_{20}O_4$ deduced from HRESIMS, which indicated that **9** had two more mass units than **6**. The proposed structure was supported by detailed 2D NMR analysis and further confirmed by an X-ray diffraction study (Figure 26), leading to the assignment of the relative configuration as 3*S**,7*S**,11*R**.

The B3LYP/6-31G(d) in vacuo, B3LYP/TZVP PCM/MeCN, and B97D/TZVP PCM/MeCN reoptimizations of the 95 MMFF conformers of (3*S*,7*S*,11*R*)-**9** yielded 3 (Figure 27), 5, and 4 conformers above 1%, respectively. The PBE0/TZVP in vacuo ECD of the B3LYP/6-31G(d) optimized low-energy conformers were in acceptable agreement with the experimental solution ECD spectrum (Figure 28), while the other two ECD levels for the same conformers gave fairly good agreement that the application of a larger basis set or advanced functional to the optimization reduced the agreement. Thus, the Boltzmann distribution computed from the B3LYP/6-31G(d) in vacuo energies should be closer to the real distribution than those obtained from the other two methods. The calculations allowed the assignment of the absolute configuration of **9** as 3*S*,7*S*,11*R*.

Dendrodolide J (**10**) was isolated as an optically active, colorless oil with a molecular formula of $C_{12}H_{20}O_4$, as established by HRESIMS. Similar to **9** vs **6**, the ^1H and ^{13}C NMR spectra of **10** (Tables 4 and 5) resembled those of **7**, with the exception of the absence of the signals for Δ^8. NOE measurements determined the relative configuration as (3*S**,7*R**,11*R**)-**10**. The B3LYP/6-31G(d) in vacuo, B3LYP/TZVP PCM/MeCN, and B97D/TZVP PCM/MeCN reoptimizations of the 30 initial MMFF conformers of (3*S*,7*R*,11*R*)- **10**

dx.doi.org/10.1021/jo400861j | J. Org. Chem. 2013, 78, 7030−7047

Table 4. ^{1}H NMR Spectroscopic Data for Dendrodolides I–M (9–13)[a]

no.	9	10	11	12	13
2	2.70 (dd, 13.2, 4.2)	2.70 (dd, 14.5, 4.5)[b]	2.51 (dd, 12.8, 4.8)[b]	2.47 (dd, 14.0, 7.6)	2.62 (dd, 15.6, 3.2)[b]
	2.54 (dd, 13.2, 3.6)	2.54 (dd, 14.5, 3.0)[c]	2.70 (dd, 12.8, 3.0)[c]	2.72 (dd, 14.0, 3.6)	2.67 (dd, 15.6, 5.2)[c]
3	4.55 (br s)	4.57 (s)	4.55 (m)	4.00 (br s)	4.09 (m)
4	5.60 (ov)	5.41 (d, 16.5)	5.56 (ddd, 15.0, 2.0, 2.0)	1.28 (td, 14.2, 7.6)	1.39 (ddd, 14.4, 9.6, 2.4)[b]
				1.55 (m)	1.82 (ddd, 14.4, 10.0, 6.0)[c]
5	5.59 (ov)	5.83 (dd, 16.5, 11.5)	5.85 (dddd, 15.0, 11.0, 4.0, 2.0)	1.70 (m)	3.61 (m)
				1.89 (m)	
6	2.21 (m)	2.44 (br d, 15.5)[b]	2.50 (ov)[b]	2.17 (ddd, 12.0, 8.5, 4.0)	3.02 (dd, 13.2, 4.3)[b]
	2.51 (m)	2.29 (ddd, 15.5, 11.5, 3.0)[c]	2.45 (ddd, 14.5, 11.0, 3.4)[c]	2.78 (ddd, 12.0, 9.2, 4.0)	2.29 (dd, 13.2, 10.8)[c]
7	4.03 (m)	3.81 (m)	4.20 (m)		
8	1.36 (m)	1.35 (m)[b]	1.46 (m)[b]	2.20 (ddd, 16.0, 8.0, 4.0)	5.26 (d, 16.0)
	1.47 (m)	1.35 (m)[c]	1.66 (ddd, 12.5, 10.5, 2.0)[c]	2.86 (ddd, 16.0, 9.0, 4.0)	
9	1.44 (m)	1.16 (m)[b]	3.72 (m)	1.77 (m)	6.43 (ddd, 16.0, 10.8, 4.8)
	1.48 (m)	1.40 (m)[c]		1.86 (m)	
10	1.70 (m)	1.68 (dd, 7.5, 7.5)[b]	2.01 (ddd, 13.5, 12.5, 4.3)[b]	1.54 (m)	2.21 (ddd, 12.0, 11.2, 2.0)[b]
	1.47 (m)	1.46 (m)[c]	1.50 (ddd, 13.5, 10.5, 3.0)[c]	1.69 (m)	2.49 (ddd, 12.0, 3.6, 1.6)[c]
11	5.14 (m)	5.12 (m)	5.11 (m)	5.19 (m)	5.25 (m)
12	1.21 (d, 6.0)	1.20 (d, 6.0)	1.23 (d, 6.0)	1.22 (d, 6.6)	1.33 (d, 6.4)
OMe					3.38 (s)

[a]In $CDCl_3$; assignments made by DEPT, ^{1}H–^{1}H COSY, HMQC, HMBC, and NOESY experiments. Values are given in ppm, with multiplicities and coupling constants (in Hz) given in parentheses. [b]α-orientation. [c]β-orientation.

Table 5. ^{13}C NMR Spectroscopic Data for Dendrodolides I–M (9–13)[a]

no.	9	10	11	12	13
1	172.4 (C)	171.9 (C)	171.7 (C)	171.9 (C)	171.5 (C)
2	41.8 (CH_2)	41.9 (CH_2)	41.8 (CH_2)	42.0 (CH_2)	39.1 (CH_2)
3	67.9 (CH)	68.0 (CH)	67.9 (CH)	67.3 (CH)	66.1 (CH)
4	133.6 (CH)	133.9 (CH)	134.6 (CH)	34.2 (CH_2)	40.0 (CH_2)
5	124.8 (CH)	123.1 (CH)	123.3 (CH)	20.2 (CH_2)	75.6 (CH)
6	38.8 (CH_2)	38.1 (CH_2)	37.9 (CH_2)	39.8 (CH_2)	46.5 (CH_2)
7	69.4 (CH)	69.7 (CH)	67.1 (CH)	211.4 (C)	198.5 (C)
8	32.3 (CH_2)	32.6 (CH_2)	39.7 (CH_2)	40.7 (CH_2)	133.3 (CH)
9	15.1 (CH_2)	19.1 (CH_2)	65.7 (CH)	17.6 (CH_2)	140.7 (CH)
10	34.3 (CH_2)	34.3 (CH_2)	44.2 (CH_2)	31.6 (CH_2)	40.1 (CH_2)
11	68.8 (CH)	68.3 (CH)	68.2 (CH)	71.0 (CH)	69.4 (CH)
12	21.1 (CH_3)	21.0 (CH_3)	21.1 (CH_3)	18.2 (CH_3)	20.6 (CH_3)
OMe					56.4 (CH_3)

[a]In $CDCl_3$; assignments made by DEPT, ^{1}H–^{1}H COSY, HMQC, HMBC, and NOESY experiments. Values are given in ppm, with assignments given in parentheses.

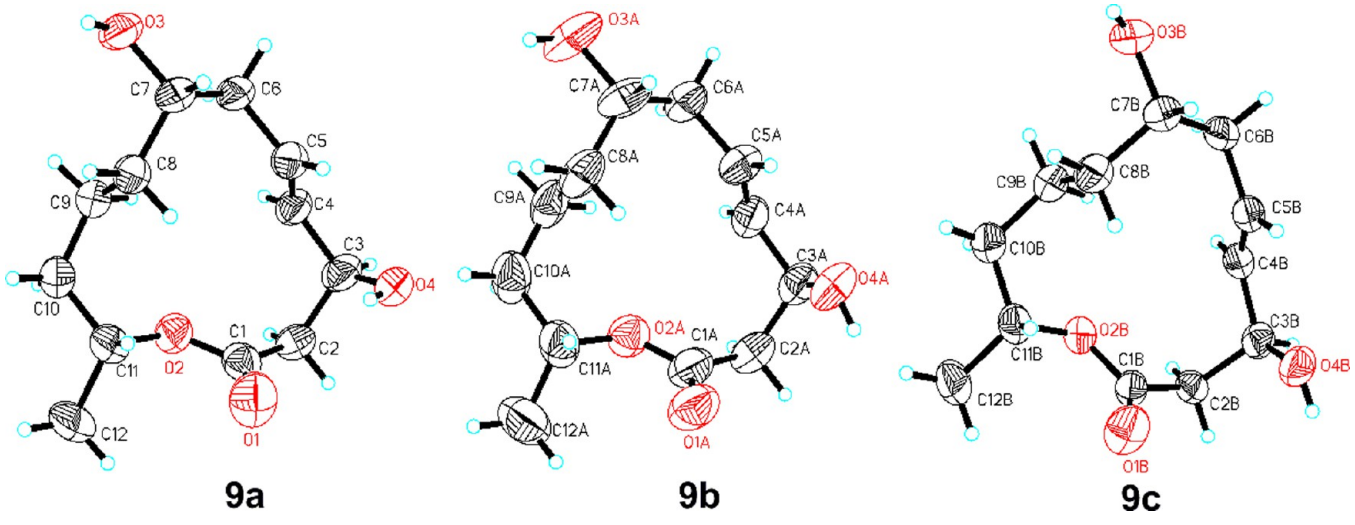

Figure 26. Single-crystal X-ray structures of **9a–c** (ORTEP drawing).

dx.doi.org/10.1021/jo400861j | J. Org. Chem. 2013, 78, 7030–7047

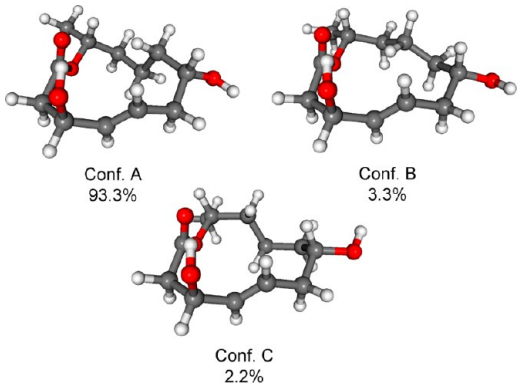

Figure 27. B3LYP/6-31G(d) in vacuo reoptimized low-energy conformers (≥1%) of (3*S*,7*S*,11*R*)-**9**.

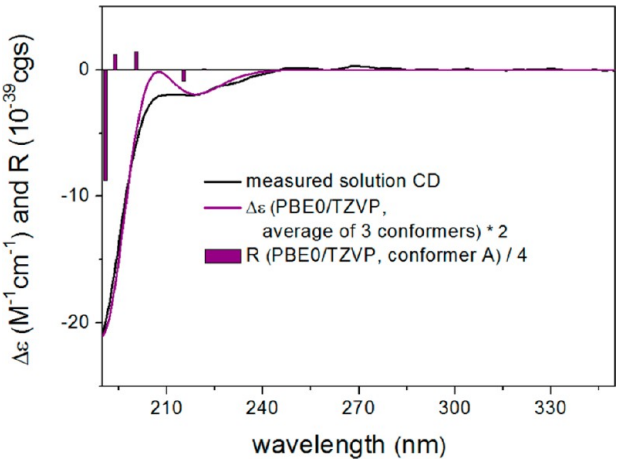

Figure 28. Experimental and Boltzmann-averaged ECD spectra of (3*S*,7*S*,11*R*)-**9** (optimization level B3LYP/6-31G(d) in vacuo, ECD level PBE0/TZVP in vacuo). Bars represent rotational strength values of the lowest energy conformer.

yielded 1, 4, and 2 (Figure 29) conformers above 1%, respectively. In the in vacuo ECD calculations, only the

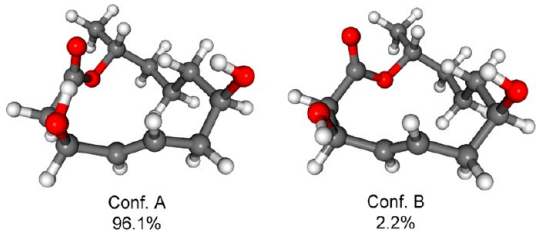

Figure 29. B97D/TZVP PCM/MeCN reoptimized low-energy conformers (≥1%) of (3*S*,7*R*,11*R*)-**10**.

B3LYP/TZVP method gave good agreement; improving the basis set, applying a solvent model, and using an advanced functional for the PBE0 optimization method also gave fairly good results (Figure 30). However, conformer B from the B97D/TZVP solvent model optimization and conformers B–D from the B3LYP/TZVP solvent model optimization give better agreement at most levels applied for the ECD calculations. This suggests that the Boltzmann population of conformer A must be somewhat lower than that estimated by any of the three levels applied for the optimization. On the basis of the good

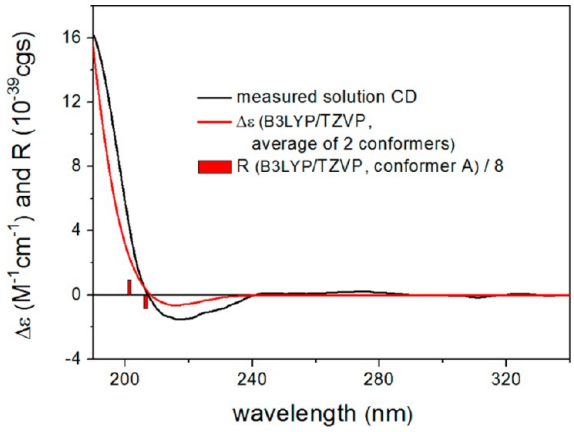

Figure 30. Experimental and Boltzmann-averaged ECD spectra of (3*S*,7*R*,11*R*)-**10** (optimization level B97D/TZVP with PCM for MeCN, ECD level B3LYP/TZVP with PCM for MeCN). Bars represent rotational strength values of the lowest energy conformer.

agreement calculated at the B3LYP ECD levels the absolute configuration of **10** was assigned as 3*S*,7*R*,11*R*.

The absolute configurations of the secondary hydroxyl groups were further confirmed by the modified Mosher method on the MPA diesters as 3*S*,7*R* (Figure 31).[73] Dendrodolide J (**10**) was then determined as the C-7 epimer of **9**.

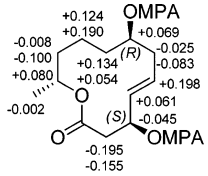

Figure 31. $\Delta\delta^{R\text{-}S}$ values (in ppm) for the MPA diesters of **10**.

Dendrodolide K (**11**), an optically active colorless oil, was assigned the molecular formula $C_{12}H_{20}O_5$ on the basis of the HRESIMS data. The structure of **11** differed from that of **10** only in the presence of an additional hydroxy group (δ_C 65.7 and δ_H 3.72; Tables 4 and 5). The location of the hydroxyl group at C-9 was readily deduced from the $^1H-^1H$ COSY and HMBC experiments. The α orientation of H-9 was deduced from the obvious NOE correlation of H-9 with H-7. This was in agreement with the absence of an NOE effect between H-9 and H-11. The relative configurations of the other asymmetric centers were same as those of **10**, on the basis of further interpretation of the NOESY experiment. The established relative configuration of the hydroxyl groups at C-7 and C-9 was further confirmed by preparation of its acetonide derivative with acetone, triethyl orthoformate, and *p*-toluenesulfonic acid in anhydrous DCM.[78] The analysis of ^1H NMR, COSY, HMQC, and NOESY spectra permitted the assignment of the two acetonide methyl groups as an axial methyl (δ_H 1.38 and δ_C 19.3) and an equatorial methyl (δ_H 1.26 and δ_C 29.9), respectively. The 1,3-diol at C-7 and C-9 was therefore in a *syn* configuration on the basis of Rychnovsky's method.[79,80] Therefore, the relative configuration of **11** was established as 3*S**,7*S**,9*S**,11*R**. The B3LYP/6-31G(d) in vacuo and B97D/TZVP PCM/MeCN reoptimizations of the 32 MMFF conformers of (3*S*,7*S*,9*S*,11*R*)-**11** yielded 1 and 2 (Figure 32) conformers above 1%, respectively. Similar to the case for **10**,

dx.doi.org/10.1021/jo400861j | J. Org. Chem. 2013, 78, 7030–7047

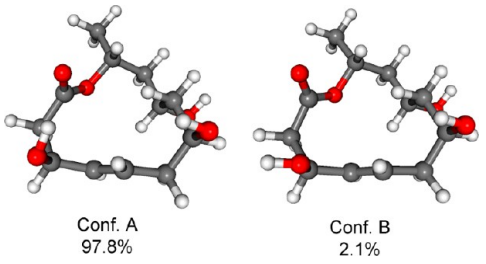

Figure 32. B97D/TZVP PCM/MeCN reoptimized low-energy conformers (≥1%) of (3*S*,7*S*,9*S*,11*R*)-**11**.

only B3LYP/TZVP represented the experimental spectrum well in the in vacuo ECD calculations (Figure 33). In this case,

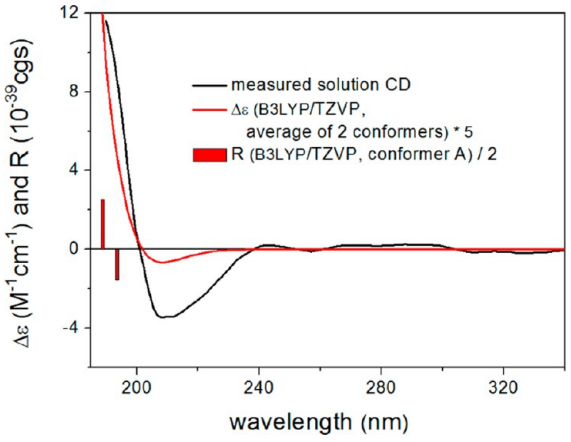

Figure 33. Experimental and Boltzmann-averaged ECD spectra of (3*S*,7*S*,9*S*,11*R*)-**11** (optimization level B97D/TZVP with PCM for MeCN, ECD level B3LYP/TZVP with PCM for MeCN). Bars represent rotational strength values of the lowest energy conformer.

improving the basis set, applying a solvent model, and using a newer type of functional did not have much effect on the overall spectra. However, similar to the case for **10**, the ECD spectra of conformer B from the B97D/TZVP solvent model calculations were in good agreement with all levels applied for the ECD calculations. Thus, the Boltzmann population of conformer B is most likely higher than that estimated by the two methods used for optimization. On the basis of the good agreement calculated at B3LYP ECD levels, the absolute configuration of **11** was assigned as 3*S*,7*S*,9*S*,11*R*.

Dendrodolide L (**12**) was obtained as needle-shaped, colorless crystals. HRESIMS data established a molecular formula of $C_{13}H_{20}O_5$, indicating that **12** has 4 fewer mass units than **5**. This was in agreement with the absence of olefinic downfield resonances in the ^{1}H and ^{13}C spectra, indicating the saturation of both the Δ^4 and Δ^8 double bonds in the structure (Tables 4 and 5). The proposed planar structure of **12** was supported by detailed analysis of the 2D NMR spectra. Its relative configuration of (3*R**,11*R**)-**12** was finally established by an X-ray diffraction study (Figure 34), because the overlapped proton signals and flexibility of the macrolide ring hindered stereochemical determination by NOESY analysis. The B3LYP/6-31G(d) in vacuo and B97D/TZVP PCM/MeCN reoptimizations of the 148 MMFF conformers of **12** yielded 8 and 11 conformers above 1% (Figure 35 and Figures

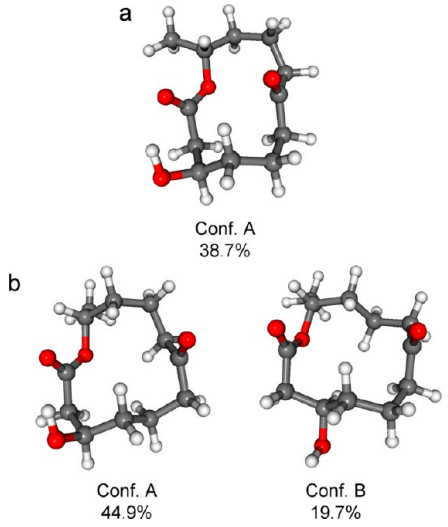

Figure 35. Lowest energy conformers giving different ECD spectra at all the applied ECD levels: (a) B3LYP/6-31G(d) in vacuo conformer A (giving mirror-image spectra); (b) B97D/TZVP PCM/MeCN conformers A (giving identical spectra except for the highest transition) and B (giving nearly identical spectra) of (3*R*,11*R*)-**12**.

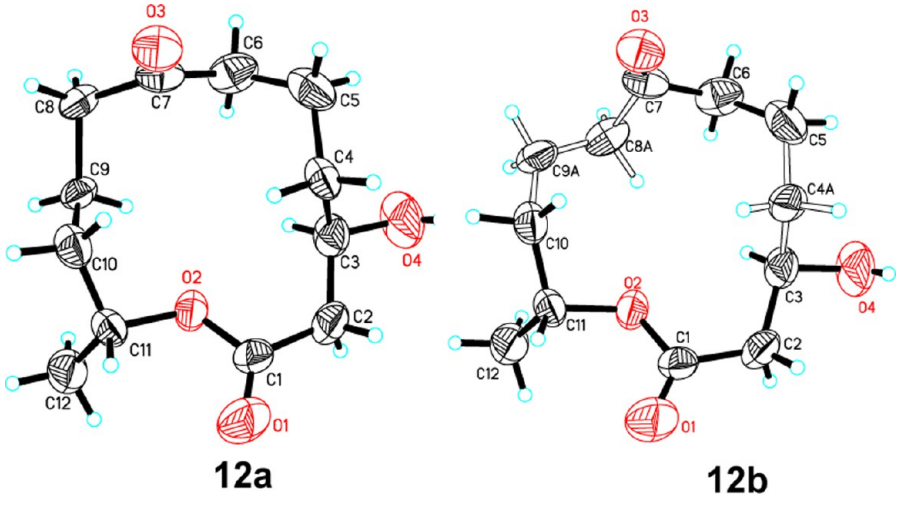

Figure 34. Single-crystal X-ray structures of **12a**,**b** (ORTEP drawing).

dx.doi.org/10.1021/jo400861j | *J. Org. Chem.* 2013, 78, 7030−7047

S8 and S9 (Supporting Information)), respectively, adequately representing the high flexibility of the molecule. The Boltzmann-averaged ECD spectra calculated for the in vacuo conformers of the 3*R*,11*R* absolute configuration are the mirror image of the experimental ECD spectrum at all levels applied for the ECD calculations. Comparison of the low-energy conformers with the X-ray structure, however, revealed that the first few low-energy conformers are quite different from the X-ray structure. The ECD spectra of conformers that were more similar to the X-ray structure (which had rather low populations) reproduced well the experimental ECD. The solvent model calculations achieved better results because they predicted well the two high-energy ECD transitions but gave opposite CE values for the 290 nm transition (Figure 36). This

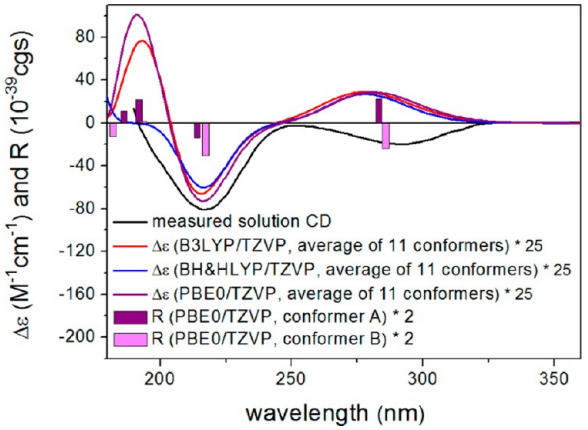

Figure 36. Experimental and Boltzmann-averaged ECD spectra of (3*R*,11*R*)-**12** (optimization level B97D/TZVP with PCM for MeCN). Bars represent rotational strength values of conformers A (purple) and B (light magenta).

improvement is due to the increase in the population of conformers with geometries similar to the X-ray geometry. In comparison to conformer B, the population of the conformers with geometries similar to the X-ray geometry (e.g., conformer B) that reproduced well the experimental ECD is still underestimated and/or the 290 nm transition is overestimated in conformer A. Although the TDDFT ECD calculations could not afford perfect agreement, on the basis of biogenetic considerations, the absolute configuration of **12** may be assigned as 3*R*,11*R*.

Dendrodolide M (**13**), an optically active, colorless oil, was assigned the molecular formula $C_{13}H_{20}O_5$ on the basis of HRESIMS and NMR data. The overall ^{1}H and ^{13}C spectra of **13** (Tables 4 and 5) resembled those of **5**, with the exception of the absence of the Δ^4 double bond and the presence of a methoxy group (δ_C 56.4, δ_H 3.38 (s)). The proton connection from H_2-2 to H_2-6 as deduced from ^{1}H−^{1}H COSY and HMBC correlation from OMe to C-5 readily located the methoxy group at C-5 and subsequently established the gross structure of **13**. An α configuration of H-5 was indicated by its NOE effects with H-2α, H-3, and H-8, whereas the β configuration of H-11 remained intact due to its NOE effect with H-9 (Figure 37). The B3LYP/6-31G(d) in vacuo and B97D/TZVP PCM/MeCN reoptimizations of the 77 MMFF conformers of (3*R*,5*S*,11*R*)-**13** yielded 2 (Figure 38) and 7 conformers above 1%, respectively. The Boltzmann-averaged ECD spectra calculated for the different sets of conformers reproduced well the three ECD transitions of the experimental spectrum (Figure

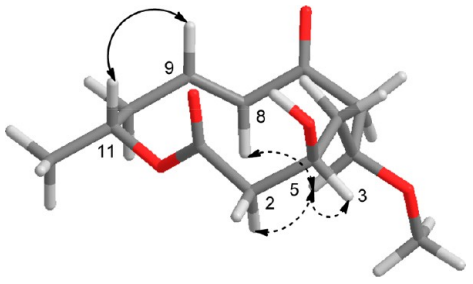

Figure 37. Key NOE correlations of **13**.

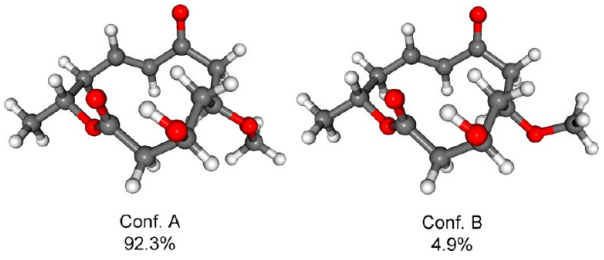

Figure 38. B3LYP/6-31G(d) in vacuo reoptimized low-energy conformers (≥1%) of (3*R*,5*S*,11*R*)-**13**.

39), enabling the unambiguous assignment of the absolute configuration of **13** as 3*R*,5*S*,11*R*.

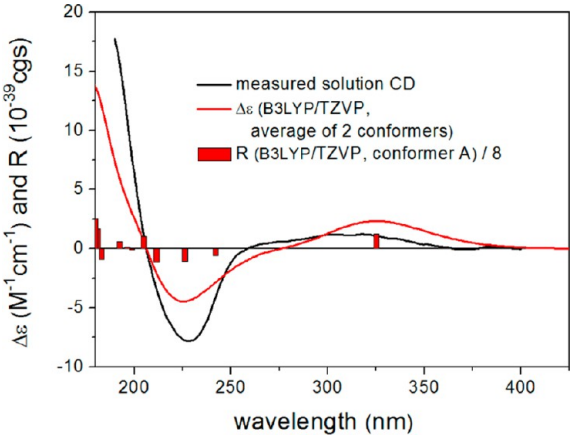

Figure 39. Experimental and Boltzmann-averaged ECD spectra of (3*R*,5*S*,11*R*)-**13** (optimization level B3LYP/6-31G(d) in vacuo, ECD level B3LYP/TZVP in vacuo). Bars represent rotational strength values of the lowest energy conformer.

The cytotoxic activity of compounds **1**−**13** toward the tumor cell lines SMMC-7721, HCT116, and A549 were evaluated in vitro (Table S2, Supporting Information). Compounds **1**−**5**, **7**−**9**, **11**, and **12** exhibited different levels of growth inhibitory activity against SMMC-7721 and HCT116 cells. No activity against A549 cells was observed (IC_{50} > 50 μg/mL).

The discovery of dendrodolides demonstrates the productivity of this fungus. The structures of dendrodolides A−K share a C3(OH)−C4=C5 subunit that has been once observed in balticolid.[17] Their chemical diversity is mainly derived from different degrees of oxidation of the 12-membered ring, particularly in the region from C-7 to C-9. Starting from the epimers of **3** and **4**, methylation on OH-9 may yield the main metabolites **1** and **2**, respectively. Reduction of the 7-keto group of **4** may yield **11**. Dehydroxylation of OH-9 in **3** and **4**

dx.doi.org/10.1021/jo400861j | J. Org. Chem. 2013, 78, 7030−7047

would give **5**. **5** may produce **12** by saturation of both Δ^4 and Δ^8 double bonds or yield **13** by the addition of water to the Δ^4 double bond and subsequent methylation. Reduction of the 7-keto group in **5** can produce **6** and **7**, which would respectively yield **9** and **10** by saturation of the Δ^8 double bond. Finally, epoxidation of the Δ^8 double bond in **7** may produce **8** (Scheme S1, Supporting Information).

Although the 12-membered-ring system is conformationally flexible, the isolation of a set of dendrodolide analogues facilitated the assignments of their relative configurations through detailed analysis of NOE effects in combination with proton coupling constants. In the low-energy conformers, the Δ^4 double bond was half circle rotated in the C-9 epimers, changing the orientations of the sp^2 methine protons: i.e., H-4β/H-5α in **1** and **3** vs H-4α/H-5β in **2** and **4**, respectively. This conformational change induced by the inversion of the C-9 chirality center produced opposite CEs in the 295 nm n–π^* and 200 nm π–π^* transitions of the β,γ-unsaturated ketone chromophore. These observations were further verified by the absolute configuration established by the modified Mosher method, X-ray crystallography, ECCD, and solution- and solid-state TDDFT ECD calculations on every isolated derivative. The conformational analysis and ECD calculations of these derivatives demonstrated that small changes in the chromophore or substitution pattern may induce significant conformational changes of the macrolide ring, which are reflected in the ECD spectra. To evaluate these changes and determine the stereochemistry, parallel use of advanced DFT methods and X-ray and NMR analysis is highly recommended.

The rarely occurring fungal polyketides, 12-membered macrolides, are acetogenic hexaketides that are cyclized in a head-to-tail fashion.[81] Biosynthetically, 12-membered macrolides are most likely generated by type I iterative highly reducing polyketide synthases (HR-PKSs), which function repeatedly by selective reduction of the keto functionalities to different extents at each cycle of chain extension to produce structurally diverse metabolites.[82] To date, the programming rules of the HR-PKS are not yet thoroughly understood.[83] As only a single β-ketoreductase is present in the iterative HP-PKS, the control mechanism for the stereochemistry of hydroxyls generated by β-ketoreduction remains obscure. Tang et al. recently reported that Hpm8, a β-ketoreductase for hypothemycin biosynthesis, exhibited stereospecificity that was controlled by the length of the growing polyketide intermediates.[84] The discovery of dendrodolides illustrates the complexity of the programming rules of iterative HR-PKSs. In addition, the coexistence of the *R* and *S* configurations among each pair of epimers, for example, 7*S* (in **6** and **9**) and 7*R* (in **7** and **10**) as well as 9*S* (in **1** and **3**) and 9*R* (in **2** and **4**), suggests that the stereospecificity control of the β-ketoreductase in the enigmatic iterative HR-PKSs is substantially more complex and far less understood.

EXPERIMENTAL SECTION

General Experimental Procedures. Precoated silica gel plates were used for analytical thin-layer chromatography (TLC). Spots were detected on TLC under UV or by heating after spraying with 0.5 mL of anisaldehyde in 50 mL of HOAc and 1 mL of H_2SO_4. TLC R_f values are reported. The NMR spectra were recorded at 293 K. Chemical shifts are reported in parts per million (δ), using the residual $CHCl_3$ signal (δ_H 7.26 ppm) as an internal standard for ^{1}H NMR and $CDCl_3$ (δ_C 77.0 ppm) for ^{13}C NMR; coupling constant (*J*) are given in Hz. ^{1}H and ^{13}C NMR assignments were supported by ^{1}H–^{1}H COSY, HMQC, HMBC, and NOESY experiments. The following abbreviations are used to describe spin multiplicity: s, singlet; d, doublet; t, triplet; q, quartet; m, multiplet; br s, broad singlet; dd, doublet of doublets; ddd, doublet of doublets of doublets; dddd, doublet of doublets of doublets of doublets; dt, doublet of triplets; qd, quartet of doublets; ov, overlapped signals. Infrared spectra were recorded in thin polymer films. For the solid-state circular dichroism (CD) protocol, see ref 85. The mass spectra and high-resolution mass spectra were performed on a Q-TOF Micro mass spectrometer, resolution 5000. An isopropyl alcohol solution of sodium iodide (2 mg/mL) was used as a reference compound. The X-ray diffraction study was carried out using Cu Kα radiation (λ = 1.54178 Å). Column chromatography (CC) was performed using silica gel (400–500 mesh) or Sephadex LH-20 ($CHCl_3$/MeOH, 2/1). Semipreparative RP-HPLC was performed using a refractive index detector and a column with 5 μm, 250 × 10 mm size with a flow rate of 1.5 mL/min.

Culture, Extraction, and Isolation. The fungus *Dendrodochium* sp. (internal strain No. 10087) was isolated from *Holothuria nobilis* Selenka, a sea cucumber collected from the South China Sea, and was cultivated on biomalt (5% w/v) solid agar medium at room temperature for 28 days.[64−66] The culture medium was extracted with acetone to afford a residue (8.0 g) after removal of the solvent under reduced pressure. The extract was subjected to column chromatography (CC) on silica gel, eluted with a gradient of MeOH in CH_2Cl_2 (1/100 to 100/1, v/v), to give 25 fractions (fractions 1–25). Fraction 16 was fractionated by Sephadex LH-20 to give **11** (3.4 mg, yield 0.43‰). Fraction 14 was first fractionated on silica gel CC (CH_2Cl_2/MeOH, 30/1) and then purified by semipreparative RP-HPLC (MeOH/H_2O, 50/50) to give **3** (1.8 mg, 30 min, yield 0.23‰), **4** (16.5 mg, 32 min, yield 2.06‰), and **5** (1.8 mg, 34 min, yield 0.23‰), respectively. Fraction 12 was fractionated on Sephadex LH-20 and then purified by semipreparative RP-HPLC (MeOH/H_2O, 25/75) to produce **6** (4.5 mg, 90 min, yield 0.56‰), **8** (1.0 mg, 120 min, yield 0.13‰), and **7** (1.4 mg, 130 min, yield 0.18‰), respectively. Fractions 9 and 10 were first purified on Sephadex LH-20 and then fractionated by semipreparative RP-HPLC (MeOH/H_2O, 30/70) to give **1** (7.4 mg, 88 min, yield 0.93‰) and **2** (41.7 mg, 102 min, yield 5.21‰). Fraction 8 was fractionated by Sephadex LH-20 followed by purification on silica gel CC (petroleum ether/acetone, 4/1) to give **12** (6.0 mg, yield 0.75‰). Fraction 7 was fractionated by Sephadex LH-20 and then purified on silica gel CC (petroleum ether/acetone, 5/1) to give **10** (29.6 mg, yield 3.7‰). Fraction 5 was purified on Sephadex LH-20 and then fractionated by semipreparative RP-HPLC (MeOH/H_2O, 35/65) to produce **9** (2.7 mg, 42 min, yield 0.34‰) and **13** (2.1 mg, 48 min, yield 0.26‰).

*Dendrodolide A (**1**):* colorless crystals (methanol); mp 115–116 °C; R_f = 0.60 (CH_2Cl_2/MeOH 9/1); $[\alpha]_D^{27.0}$ = +41.9° (*c* 0.370, $CHCl_3$); ECD (CH_3CN, *c* 3.9 × 10^{-4}) λ_{max} ($\Delta\varepsilon$) 203 (1.93), 228 (−0.55), 249 (−0.09), 296 (−1.39) nm; UV (CH_3CN) λ_{max} (ε) 280 (382) nm; IR (film) ν_{max} 3420, 2979, 2933, 1723, 1251, 1168, 1095, 976 cm^{-1}; ^{1}H and ^{13}C NMR spectroscopic data, see Tables 1 and 2; HRMS (ESI) $[M + H]^+$ *m*/*z* 257.1394 (calcd for $C_{13}H_{21}O_5$, 257.1389).

*Dendrodolide B (**2**):* colorless oil; R_f = 0.63 (CH_2Cl_2/MeOH 9/1); $[\alpha]_D^{27.0}$ = +127° (*c* 2.50, $CHCl_3$); ECD (CH_3CN, *c* 2.8 × 10^{-4}) λ_{max} ($\Delta\varepsilon$) 198 (−2.99), 220 (−0.64), 292 (4.61) nm; UV (CH_3CN) λ_{max} (ε) 230 (1426), 280 (391) nm; IR (film) ν_{max} 3502, 2979, 2934, 1712, 1261, 1168, 1089, 980 cm^{-1}; ^{1}H and ^{13}C NMR spectroscopic data, see Tables 1 and 2; HRMS (ESI) $[M + H]^+$ *m*/*z* 257.1392 (calcd for $C_{13}H_{21}O_5$, 257.1389).

*Dendrodolide C (**3**):* colorless oil; R_f = 0.53 (CH_2Cl_2/MeOH 9/1); $[\alpha]_D^{27.0}$ = +122° (*c* 0.090, $CHCl_3$); ECD (CH_3CN, *c* 3.0 × 10^{-4}) λ_{max} ($\Delta\varepsilon$) 199 (3.04), 225 (−0.88), 246 (−0.06), 295 (−1.89) nm; UV (CH_3CN) λ_{max} (ε) 270 (562) nm; IR (film) ν_{max} 3401, 2976, 2930, 1707, 1267, 1177, 1065, 973 cm^{-1}; ^{1}H and ^{13}C NMR spectroscopic data, see Tables 1 and 2; HRMS (ESI) $[M + H]^+$ *m*/*z* 243.1237 (calcd for $C_{12}H_{19}O_5$, 243.1232).

*Dendrodolide D (**4**):* colorless crystals (methanol); mp 168–169 °C; R_f = 0.56 (CH_2Cl_2/MeOH 9/1); $[\alpha]_D^{27.0}$ = +83.4° (*c* 0.825, $CHCl_3$); ECD (CH_3CN, *c* 3.9 × 10^{-4}) λ_{max} ($\Delta\varepsilon$) =199 (−4.44), 220 (−0.58), 292 (5.69) nm; UV (CH_3CN) λ_{max} (ε) 230 (1707), 284

dx.doi.org/10.1021/jo400861j | J. Org. Chem. 2013, 78, 7030−7047

(381) nm; IR (film) ν_{max} 3384, 2961, 1698, 1258, 1161, 1119, 1034, 960 cm^{-1}; ^1H and ^{13}C NMR spectroscopic data, see Tables 1 and 2; HRMS (ESI) $[M + H]^+$ m/z 243.1237 (calcd for $C_{12}H_{19}O_5$, 243.1232).

*Dendrodolide E (**5**):* colorless oil; R_f = 0.68 (CH_2Cl_2/MeOH 9/1); $[\alpha]_D^{27.0}$ = +42.7° (*c* 0.090, $CHCl_3$); ECD (CH_3CN, *c* 9.0 × 10^{-5}) λ_{max} ($\Delta\varepsilon$) 198 (2.92), 219 (−2.66), 242 (0.99), 317 (1.56) nm; UV (CH_3CN) λ_{max} (ε) 276 (2518) nm; IR (film) ν_{max} 3451, 2973, 2930, 1716, 1260, 1169, 1054, 978 cm^{-1}; ^{13}C and ^1H NMR spectroscopic data, see Tables 2 and 3; HRMS (ESI) $[M + H]^+$ m/z 225.1131 (calcd for $C_{12}H_{17}O_4$, 225.1127).

*Dendrodolide F (**6**):* colorless oil; R_f = 0.54 (CH_2Cl_2/MeOH 9/1); $[\alpha]_D^{27.0}$ = +183° (*c* 0.150, $CHCl_3$); ECD (CH_3CN, *c* 4.5 × 10^{-4}) λ_{max} ($\Delta\varepsilon$) 222 (−1.18) nm; UV (CH_3CN) λ_{max} (ε) 230 (1437) nm; IR (film) ν_{max} 3400, 2929, 1709, 1366, 1259, 1170, 1028, 962 cm^{-1}; ^{13}C and ^1H NMR spectroscopic data, see Tables 2 and 3; HRMS (ESI) $[M + H]^+$ m/z 227.1282 (calcd for $C_{12}H_{19}O_4$, 227.1283).

*Dendrodolide G (**7**):* colorless oil; R_f = 0.60 (CH_2Cl_2/MeOH 9/1); $[\alpha]_D^{27.0}$ = +59.4° (*c* 0.070, $CHCl_3$); ECD (CH_3CN, *c* 4.2 × 10^{-4}) λ_{max} ($\Delta\varepsilon$) 220 (−0.50) nm; UV (CH_3CN) λ_{max} (ε) 228 (3271) nm; IR (film) ν_{max} 3369, 2925, 1713, 1367, 1261, 1172, 1032, 962 cm^{-1}; ^{13}C and ^1H NMR spectroscopic data, see Tables 2 and 3; HRMS (ESI) $[M + H]^+$ m/z 227.1286 (calcd for $C_{12}H_{19}O_4$, 227.1283).

*Dendrodolide H (**8**):* colorless oil; R_f = 0.51 (CH_2Cl_2/MeOH 9/1); $[\alpha]_D^{27.0}$ = +41.5° (*c* 0.050, $CHCl_3$); ECD (CH_3CN, *c* 3.0 × 10^{-4}) λ_{max} ($\Delta\varepsilon$) 219 (0.47), 241 (−0.33) nm; UV (CH_3CN) λ_{max} (ε) 225 (2967) nm; IR (film) ν_{max} 3391, 2925, 1723, 1378, 1250, 1170, 1068, 984 cm^{-1}; ^{13}C and ^1H NMR spectroscopic data, see Tables 2 and 3; HRMS (ESI) $[M + Na]^+$ m/z 265.1053 (calcd for $C_{12}H_{18}O_5Na$, 265.1052).

*Dendrodolide I (**9**):* colorless crystals (methanol); mp 108−109 °C; R_f = 0.59 (CH_2Cl_2/MeOH 9/1); $[\alpha]_D^{27.0}$ = −15.9° (*c* 0.135, $CHCl_3$); ECD (CH_3CN, *c* 2.7 × 10^{-4}) λ_{max} ($\Delta\varepsilon$) 217 (−0.50) nm; UV (CH_3CN) λ_{max} (ε) 228 (1079) nm; IR (film) ν_{max} 3380, 2931, 2854, 1708, 1265, 1167, 1109, 969 cm^{-1}; ^1H and ^{13}C NMR spectroscopic data, see Tables 4 and 5; HRMS (ESI) $[M + Na]^+$ m/z 251.1261 (calcd for $C_{12}H_{20}O_4Na$, 251.1259).

*Dendrodolide J (**10**):* colorless oil; R_f = 0.51 (CH_2Cl_2/MeOH 9/1); $[\alpha]_D^{27.0}$ = +25.1° (*c* 0.945, $CHCl_3$); ECD (CH_3CN, *c* 2.7 × 10^{-4}) λ_{max} ($\Delta\varepsilon$) 217 (−0.39) nm; UV (CH_3CN) λ_{max} (ε) 230 (332) nm; IR (film) ν_{max} 3399, 2930, 2862, 1708, 1262, 1165, 1138, 977 cm^{-1}; ^1H and ^{13}C NMR spectroscopic data, see Tables 4 and 5; HRMS (ESI) $[M + H]^+$ m/z 229.1445 (calcd for $C_{12}H_{21}O_4$, 229.1440).

*Dendrodolide K (**11**):* colorless oil; R_f = 0.25 (CH_2Cl_2/MeOH 9/1); $[\alpha]_D^{27.0}$ = +11.7° (*c* 0.285, $CHCl_3$); ECD (CH_3CN, *c* 2.0 × 10^{-3}) λ_{max} ($\Delta\varepsilon$) 208 (−0.13) nm; UV (CH_3CN) λ_{max} (ε) 225 (399) nm; IR (film) ν_{max} 3355, 2925, 1715, 1264, 1168, 1139, 1074, 980 cm^{-1}; ^1H and ^{13}C NMR spectroscopic data, see Tables 4 and 5; HRMS (ESI) $[M + H]^+$ m/z 245.1392 (calcd for $C_{12}H_{21}O_5$, 245.1389).

*Dendrodolide L (**12**):* colorless crystals (methanol); mp 96−97 °C; R_f = 0.50 (CH_2Cl_2/MeOH 9/1); $[\alpha]_D^{27.0}$ = +10.7° (*c* 0.065, $CHCl_3$); ECD (CH_3CN, *c* 2.6 × 10^{-4}) λ_{max} ($\Delta\varepsilon$) 217 (−9.01), 291 (−2.23) nm; UV (CH_3CN) λ_{max} (ε) 226 (1128), 276 (257) nm; IR (film) ν_{max} 3381, 2949, 2927, 1728, 1700, 1253, 1189, 979 cm^{-1}; ^1H and ^{13}C NMR spectroscopic data, see Tables 4 and 5; HRMS (ESI) $[M + NH_4]^+$ m/z 246.1712 (calcd for $C_{12}H_{24}NO_4$, 246.1705).

*Dendrodolide M (**13**):* colorless oil; R_f = 0.67 (CH_2Cl_2/MeOH 9/1); $[\alpha]_D^{27.0}$ = +92.6° (*c* 0.105, $CHCl_3$); ECD (CH_3CN, *c* 4.2 × 10^{-4}) λ_{max} ($\Delta\varepsilon$) 228 (−1.44), 318 (0.23) nm; UV (CH_3CN) λ_{max} (ε) 220 (5179) nm; IR (film) ν_{max} 3491, 2971, 1726, 1691, 1270, 1167, 1094, 983 cm^{-1}; ^1H and ^{13}C NMR spectroscopic data, see Tables 4 and 5; HRMS (ESI) $[M + H]^+$ m/z 257.1395 (calcd for $C_{13}H_{21}O_5$, 257.1389).

X-ray Crystallographic Studies of Dendrodolide A (1). A colorless needle-shaped crystal of **1** (0.20 × 0.10 × 0.10 mm) was obtained by recrystallization from MeOH: $C_{13}H_{20}O_5$ (M_r = 256.29), orthorhombic, space group $P2_12_12_1$ with *a* = 7.6430(15) Å, *b* = 11.316(2) Å, *c* = 15.823(3) Å, $\alpha = \beta = \gamma$ = 90.00°, *V* = 1368.5(5) $Å^3$, *Z* = 4, and D_{calcd} = 1.244 g/cm^3. Intensity data were measured using Cu Kα radiation (graphite monochromator). A total of 6415 reflections were collected to a maximum 2θ value of 133.7° at 296(2) K. The structures were solved by direct methods (SHELXS-97) and refined using full-matrix least-squares difference Fourier techniques. All non-hydrogen atoms were given anisotropic thermal parameters; hydrogen atoms were located from difference Fourier maps and refined at idealized positions riding on their parent atoms. The refinement converged at R1($I > 2\sigma(I)$) = 0.0347 and wR2 = 0.0913 for 2335 independent reflections and 163 variables; absolute structure parameter −0.1(2).

X-ray Crystallographic Studies of Dendrodolide D (4). A colorless needle-shaped crystal of **4** (0.25 × 0.08 × 0.08 mm) was obtained by recrystallization from MeOH: $C_{12}H_{18}O_5$ (M_r = 242.26), monoclinic, space group $P2_1$ with *a* = 7.2552(15) Å, α = 90.00°, *b* = 5.7296(11) Å, β = 98.35°, *c* = 14.708(3) Å, γ = 90.00°, *V* = 604.9(2) $Å^3$, *Z* = 2, and D_{calcd} = 1.330 g/cm^3. Intensity data were measured using Cu Kα radiation (graphite monochromator). A total of 3413 reflections were collected to a maximum 2θ value of 133.78° at 296(2) K. The structures were solved by direct methods (SHELXS-97) and refined using full-matrix least-squares difference Fourier techniques. All non-hydrogen atoms were given anisotropic thermal parameters; hydrogen atoms were located from difference Fourier maps and refined at idealized positions riding on their parent atoms. The refinement converged at R1($I > 2\sigma(I)$) = 0.0576 and wR2 = 0.1474 for 1767 independent reflections and 154 variables; absolute structure parameter −0.2(3).

X-ray Crystallographic Studies of Dendrodolide I (9). A colorless needle-shaped crystal of **9** (0.20 × 0.08 × 0.07 mm) was obtained by recrystallization from MeOH: $C_{12}H_{20}O_4$ (M_r = 228.28), orthorhombic, space group $P2_12_12_1$ with *a* = 5.336 Å, *b* = 25.071 Å, *c* = 29.472 Å, $\alpha = \beta = \gamma$ = 90.00°, *V* = 3942.7 $Å^3$, *Z* = 12, and D_{calcd} = 1.154 g/cm^3. Intensity data were measured using Cu Kα radiation (graphite monochromator). A total of 13191 reflections were collected to a maximum 2θ value of 133.98° at 296(2) K. The structures were solved by direct methods (SHELXS-97) and refined using full-matrix least-squares difference Fourier techniques. All non-hydrogen atoms were given anisotropic thermal parameters; hydrogen atoms were located from difference Fourier maps and refined at idealized positions riding on their parent atoms. The refinement converged at R1($I > 2\sigma(I)$) = 0.0750 and wR2 = 0.1743 for 6050 independent reflections and 434 variables; absolute structure parameter 0.2(4). There are three title compounds in the asymmetric unit, leading to the larger unit cell parameters. A serial O−H···O hydrogen bond can be found between adjacent title compounds.

X-ray Crystallographic Studies of Dendrodolide L (12). A colorless needle-shaped crystal of **12** (0.30 × 0.08 × 0.08 mm) was obtained by recrystallization from MeOH: $C_{12}H_{20}O_4$ (M_r = 228.28), monoclinic, space group $P2_1$ with *a* = 8.5350(10) Å, α = 90.00°, *b* = 5.5710(10) Å, β = 91.78°, *c* = 13.1410 (10) Å, γ = 90.00°, *V* = 624.53(14) $Å^3$, *Z* = 2, and D_{calcd} = 1.214 g/cm^3. Intensity data were measured using Cu Kα radiation (graphite monochromator). A total of 3935 reflections were collected to a maximum 2θ value of 133.56° at 296(2) K. The structures were solved by direct methods (SHELXS-97) and refined using full-matrix least-squares difference Fourier techniques. All non-hydrogen atoms were given anisotropic thermal parameters; hydrogen atoms were located from difference Fourier maps and refined at idealized positions riding on their parent atoms. The refinement converged at R1($I > 2\sigma(I)$) = 0.0707 and wR2 = 0.2167 for 2032 independent reflections and 173 variables; absolute structure parameter −0.2(5). There are hydrogen bonds between O4−H4A···O4 (symmetry operation A: $-x, y + {}^1/_2, -z + 1$), forming one-dimension Z-shaped chains along the *b* axis. Methylenes at C-8 and C-9 exhibit positional disorder because of the rotation of single bonds.

Esterification of Dendrodolide B (2) with (*R*)-MPA Acid. Treating **2** (0.90 mg) with (*R*)-MPA acid (1.20 mg), DMAP (1.08 mg), and EDC (1.35 mg) in dry DCM (1.0 mL), stirring at room temperature overnight, and purifying by mini silica gel column chromatography (500 mesh, petroleum ether/ethyl acetate, 7/2) afforded the (*R*)-MPA ester of **2** (0.92 mg, 65%): ^1H NMR (500 MHz, $CDCl_3$, 25 °C) δ 5.73 (m, 1H, H-4), 5.73 (m, 1H, H-5), 5.57 (m, 1H, H-3), 5.00 (m, 1H, H-11), 3.92 (m, 1H, H-9), 3.31 (s, 3H,

dx.doi.org/10.1021/jo400861j | J. Org. Chem. 2013, 78, 7030−7047

OMe), 3.16 (dd, J = 14.0, 7.7 Hz, 1H, H-6α), 3.05 (dd, J = 14.0, 6.4 Hz, 1H, H-6β), 2.75 (dd, J = 14.5, 5.9 Hz, 1H, H-8β), 2.65 (dd, J = 14.3, 4.3 Hz, 1H, H-2β), 2.58 (dd, J = 14.3, 6.6 Hz, 1H, H-2α), 2.34 (dd, J = 14.5, 8.0 Hz, 1H, H-8α), 1.94 (ddd, J = 14.5, 9.7, 3.7 Hz, 1H, H-10α), 1.61 (ddd, J = 14.5, 8.0, 2.6 Hz, 1H, H-10β), 1.24 (d, J = 6.2 Hz, 3H, H-12); ^{1}H NMR (500 MHz, $CDCl_3$, −25 °C) δ 5.78 (dd, J = 15.5, 4.4 Hz, 1H, H-4), 5.68 (m, 1H, H-5), 5.60 (br d, J = 3.3 Hz, 1H, H-3), 4.93 (br s, 1H, H-11), 3.93 (m, 1H, H-9), 3.33 (s, 3H, OMe), 3.18 (dd, J = 14.3, 9.3 Hz, 1H, H-6α), 3.06 (dd, J = 14.3, 5.6 Hz, 1H, H-6β), 2.75 (dd, J = 14.0, 4.6 Hz, 1H, H-8β), 2.64 (dd, J = 14.0, 3.9 Hz, 1H, H-2β), 2.54 (dd, J = 14.0, 6.1 Hz, 1H, H-2α), 2.27 (dd, J = 14.0, 9.1 Hz, 1H, H-8α), 2.03 (m, 1H, H-10α), 1.52 (m, 1H, H-10β), 1.23 (d, J = 6.1 Hz, 3H, H-12).

Esterification of Dendrodolide B (2) with *p*-Methoxybenzoic Acid. The same reaction of **2** (1.00 mg) with *p*-methoxybenzoic acid (1.19 mg), DMAP (1.20 mg), and EDC (1.50 mg) afforded the *p*-methoxybenzoate of **2** (0.94 mg, 62%): ^{1}H NMR (500 MHz, $CDCl_3$) δ 5.88 (dd, J = 15.4, 3.9 Hz, 1H, H-5), 5.80 (m, 1H, H-4), 5.79 (m, 1H, H-3), 5.01 (m, 1H, H-11), 4.01 (m, 1H, H-9), 3.87 (s, 3H, OMe), 3.22 (dd, J = 14.8, 9.4 Hz, 1H, H-6α), 3.07 (dd, J = 14.8, 5.5 Hz, 1H, H-6β), 2.89 (dd, J = 13.5, 5.6 Hz, 1H, H-2β), 2.79 (dd, J = 13.5, 3.4 Hz, 1H, H-2α), 2.78 (dd, J = 14.2, 4.5 Hz, 1H, H-8β), 2.34 (dd, J = 14.2, 9.1 Hz, 1H, H-8α), 2.06 (ddd, J = 14.4, 10.4, 3.9 Hz, 1H, H-10α), 1.58 (ddd, J = 14.4, 8.7, 2.9 Hz, 1H, H-10β), 1.29 (d, J = 6.2 Hz, 3H, H-12).

Esterification of Dendrodolide F (6) with (*R*)-MPA Acid. The same reaction of **6** (0.67 mg) with (*R*)-MPA acid (1.95 mg), DMAP (0.90 mg), and EDC (1.20 mg) afforded the (*R*)-MPA diester of **6** (1.02 mg, 66%): ^{1}H NMR (500 MHz, $CDCl_3$) δ 5.47 (ov, 1H, H-3), 5.44 (ov, 1H, H-5), 5.36 (dd, J = 15.3, 5.4 Hz, 1H, H-4), 5.27 (m, 1H, H-7), 5.21 (ddd, J = 15.0, 8.4, 3.9 Hz, 1H, H-9), 5.06 (dd, J = 15.0, 7.7 Hz, 1H, H-8), 4.95 (m, 1H, H-11), 2.53 (dd, J = 14.3, 6.8 Hz, 1H, H-2β), 2.49 (dd, J = 14.3, 3.9 Hz, 1H, H-2α), 2.43 (m, 1H, H-6β), 2.34 (br d, J = 14.3 Hz, 1H, H-10β), 2.24 (ddd, J = 12.9, 8.5, 8.5 Hz, 1H, H-6α), 1.99 (ddd, J = 14.3, 8.9, 8.9 Hz, 1H, H-10α), 1.13 (d, J = 6.4 Hz, 3H, H-12).

Esterification of Dendrodolide F (6) with (*S*)-MPA Acid. The same reaction of **6** (0.67 mg) with (*S*)-MPA acid (1.95 mg) afforded the (*S*)-MPA diester of **6** (0.86 mg, 56%): ^{1}H NMR (500 MHz, $CDCl_3$) δ 5.42 (br s, 1H, H-3), 5.31 (ddd, J = 15.0, 7.0, 3.3 Hz, 1H, H-9), 5.17 (dd, J = 15.6, 3.3 Hz, 1H, H-4), 5.11 (dd, J = 15.0, 8.8 Hz, 1H, H-8), 4.98 (m, 1H, H-11), 4.95 (m, 1H, H-7), 4.61 (m, 1H, H-5), 2.79 (dd, J = 13.5, 6.2 Hz, 1H, H-2β), 2.48 (dd, J = 13.5, 2.8 Hz, 1H, H-2α), 2.32 (br d, J = 14.7 Hz, 1H, H-10β), 2.09 (m, 1H, H-10α), 2.05 (m, 1H, H-6β), 1.83 (dd, J = 16.0, 10.6 Hz, 1H, H-6α), 1.22 (d, J = 6.2 Hz, 3H, H-12).

Esterification of Dendrodolide J (10) with (*R*)-MPA Acid. The same reaction of **10** (0.60 mg) with (*R*)-MPA acid (1.8 mg) afforded the (*R*)-MPA diester of **10** (0.83 mg, 60%): ^{1}H NMR (400 MHz, $CDCl_3$) δ 5.65 (m, 1H, H-5), 5.52 (m, 1H, H-4), 5.50 (m, 1H, H-3), 4.94 (m, 1H, H-7), 4.91 (m, 1H, H-11), 2.59 (dd, J = 13.8, 4.2 Hz, 1H, H-2α), 2.47 (dd, J = 13.8, 6.2 Hz, 1H, H-2β), 2.29 (ddd, J = 11.6, 8.2, 3.3 Hz, 1H, H-6α), 2.16 (m, 1H, H-6β), 1.59 (m, 1H, H-10α), 1.52 (m, 1H, H-8β), 1.50 (m, 1H, H-10β), 1.45 (m, 1H, H-9β), 1.43 (m, 1H, H-9α), 1.29 (m, 1H, H-8α), 1.18 (d, J = 6.2 Hz, 3H, H-12).

Esterification of Dendrodolide J (10) with (*S*)-MPA Acid. The same reaction of **10** (0.70 mg) with (*S*)-MPA acid (2.00 mg) afforded the (*S*)-MPA diester of **10** (0.88 mg, 55%): ^{1}H NMR (500 MHz, $CDCl_3$) δ 5.55 (m, 1H, H-3), 5.45 (m, 1H, H-5), 5.46 (m, 1H, H-4), 4.87 (m, 1H, H-7), 4.83 (m, 1H, H-11), 2.78 (dd, J = 13.5, 5.9 Hz, 1H, H-2α), 2.62 (dd, J = 13.5, 3.8 Hz, 1H, H-2β), 2.31 (ddd, J = 11.2, 6.9, 3.2 Hz, 1H, H-6α), 2.25 (m, 1H, H-6β), 1.60 (m, 2H, H-10), 1.38 (m, 1H, H-8β), 1.33 (m, 1H, H-9β), 1.24 (m, 1H, H-8α), 1.24 (m, 1H, H-9α), 1.18 (d, J = 6.1 Hz, 3H, H-12).

Acetonide of Dendrodolide K (11). Dendrodolide K (**11**, 1.4 mg) was dissolved in anhydrous DCM (0.5 mL), and acetone (2.0 μL), triethyl orthoformate (2.0 μL), and *p*-toluenesulfonic acid (0.1 mg) were added. The reaction mixture was stirred for 3 h at room temperature and then quenched with 5% aqueous $NaHCO_3$, and the solvent was removed under reduced pressure. The purification was performed on a mini silica gel CC (500 mesh, petroleum ether/acetone, 8/1) to provide the acetonide of **11** (0.5 mg, 31%): ^{1}H NMR (600 MHz, acetone-d_6) δ 5.64 (m, 1H, H-11), 5.61 (m, 1H, H-5), 5.51 (dd, J = 16.3, 3.2 Hz, 1H, H-4), 4.49 (m, 1H, H-3), 4.13, (m, 1H, H-7), 4.09 (m, 1H, H-9), 3.91 (d, J = 8.9 Hz, 1H, 3-OH), 2.67 (dd, J = 13.4, 5.6 Hz, 1H, H-2α), 2.56 (dd, J = 13.4, 2.4 Hz, 1H, H-2β), 2.45 (m, 1H, H-10β), 2.27 (ddd, J = 13.9, 12.2, 1.5 Hz,1H, H-8β), 1.84 (ddd, J = 13.2, 10.5, 2.4 Hz, 1H, H-10α), 1.72 (m, 2H, H-6), 1.38 (s, 3H, acetonide ax CH_3), 1.26 (s, 3H, acetonide eq CH_3), 1.13 (d, J = 6.5 Hz, 3H, H-12), 0.89 (ddd, J = 13.9, 4.5, 4.5 Hz, 1H, H-8α); selected ^{13}C NMR (150 MHz, acetone-d_6) δ 137.7 (C-4), 124.3 (C-5), 64.5 (C-7), 68.3 (C-3), 66.5 (C-11), 65.2 (C-9), 41.6 (C-2), 39.6 (C-6), 36.9 (C-10), 29.9 (acetonide eq CH_3), 21.8 (C-12), 34.5 (C-8), 19.3 (acetonide ax CH_3).

Cytotoxicity Assay. The cytotoxic activity of tested compounds against human hepatoma cells (SMMC-7721), human colon cancer cells (HCT116), and human lung adenocarcinoma (A549) was assayed by the MTT (3-(4,5-dimethylthiazol-2-yl)-2,5-diphenyltetrazolium bromide) colorimetric method.[86] Adriamycin was used as standard control.

Computational Details. Geometry optimizations (B3LYP/6-31G(d) in vacuo, B3LYP/TZVP with PCM model for MeCN, and B97D/TZVP[71] with PCM model for MeCN levels of theory) and TDDFT calculations were performed with Gaussian 09 using various functionals (B3LYP, BH&HLYP, PBE0) and the TZVP basis set in vacuo and with the PCM model for MeCN. CD spectra were generated as the sum of Gaussians[88] with 3000 cm^{-1} half-height width (corresponding to 27 at 300 nm), using dipole-velocity computed rotational strengths for conformers above 1%. Mixed torsional/low mode conformational searches were carried out by means of the Macromodel 9.9.223[89] software using Merck Molecular Force Field (MMFF) with implicit solvent model for chloroform applying a 21 kJ/mol energy window and generating 10.000 structures. Boltzmann distributions were estimated from the ZPVE corrected B3LYP/6-31G(d) energies in the gas-phase calculations and from the B3LYP/TZVP and B97D/TZVP energies in the PCM model calculations. The MOLEKEL[90] software package was used for visualization of the results.

■ ASSOCIATED CONTENT

Supporting Information

Text, tables, figures, and CIF files giving HRMS and one- and two-dimensional NMR spectra for compounds **1**−**13**, the low energy conformers for **1**, **3**, **7**, and **12**, crystallographic data for crystals **1**, **4**, **9**, and **12**, and atom coordinates and absolute energies of the computed structures. This material is available free of charge via the Internet at http://pubs.acs.org.

■ AUTHOR INFORMATION

Corresponding Author

*W.Z.: tel/fax, 86 21 81871257; e-mail, wenzhang1968@163.com.

Author Contributions

‖These authors contributed equally to this work.

Notes

The authors declare no competing financial interest.

■ ACKNOWLEDGMENTS

The research work was financially supported by the Natural Science Foundation of China (No. 30873200, 81202453), National Marine "863" Project (No. 2013AA092902), and the Shanghai Pujiang Program (PJ2008). T.K. and A.M. thank the Hungarian National Research Foundation (OTKA K105871) for financial support and the National Information Infrastructure Development Institute (NIIFI 10038) for CPU time.

REFERENCES

(1) Vesonder, R. F.; Stodola, F. H.; Wickerha, L. J.; Ellis, J. J.; Rohwedde, W. K. *Can. J. Chem.* **1971**, *49*, 2029−2032.
(2) Hirota, A.; Isogai, A.; Sakai, H. *Agric. Biol. Chem.* **1981**, *45*, 799−800.
(3) Hirota, A.; Sakai, H.; Isogai, A. *Agric. Biol. Chem.* **1985**, *49*, 731−735.
(4) Hirota, A.; Sakai, H.; Isogai, A.; Kitano, Y.; Ashida, T.; Hirota, H.; Takahashi, T. *Agric. Biol. Chem.* **1985**, *49*, 903−904.
(5) Hirota, H.; Hirota, A.; Sakai, H.; Isogai, A.; Takahashi, T. *Bull. Chem. Soc. Jpn.* **1985**, *58*, 2147−2148.
(6) Sekiguchi, J.; Kuroda, H.; Yamada, Y.; Okada, H. *Tetrahedron Lett.* **1985**, *26*, 2341−2342.
(7) Rodphaya, D.; Sekiguchi, J.; Yamada, Y. *J. Antibiot.* **1986**, *39*, 629−635.
(8) Fujii, Y.; Fukuda, A.; Hamasaki, T.; Ichimoto, I.; Nakajima, H. *Phytochemistry* **1995**, *40*, 1443−1446.
(9) Smith, C. J.; Abbanat, D.; Bernan, V. S.; Maiese, W. M.; Greenstein, M.; Jompa, J.; Tahir, A.; Ireland, C. M. *J. Nat. Prod.* **2000**, *63*, 142−145.
(10) Zhang, H.; Tomoda, H.; Tabata, N.; Miura, H.; Namikoshi, M.; Yamaguchi, Y.; Masuma, R.; Omura, S. *J. Antibiot.* **2001**, *54*, 635−641.
(11) Jadulco, R.; Proksch, P.; Wray, V.; Sudarsono; Berg, A.; Grafe, U. *J. Nat. Prod.* **2001**, *64*, 527−530.
(12) Shigemori, H.; Kasai, Y.; Komatsu, K.; Tsuda, M.; Mikami, Y.; Kobayashi, J. *Mar. Drugs* **2004**, *2*, 164−169.
(13) Gesner, S.; Cohen, N.; Ilan, M.; Yarden, O.; Carmeli, S. *J. Nat. Prod.* **2005**, *68*, 1350−1353.
(14) Dai, H.-Q.; Kang, Q.-J.; Li, G.-H.; Shen, Y.-M. *Helv. Chim. Acta* **2006**, *89*, 527−531.
(15) Jiao, P.; Swenson, D. C.; Gloer, J. B.; Wicklow, D. T. *J. Nat. Prod.* **2006**, *69*, 636−639.
(16) Qi, S. H.; Xu, Y.; Xiong, H. R.; Qian, P. Y.; Zhang, S. *World J. Microb. Biot.* **2009**, *25*, 399−406.
(17) Shushni, M. A. M.; Singh, R.; Mentel, R.; Lindequist, U. *Mar. Drugs* **2011**, *9*, 844−851.
(18) Corey, E. J.; Ulrich, P.; Fitzpatrick, J. M. *J. Am. Chem. Soc.* **1976**, *98*, 222−224.
(19) Chen, Q.; Du, Y. *Tetrahedron Lett.* **2006**, *47*, 8489−8492.
(20) Krishna, P. R.; Kumar, P. V. A. *Helv. Chim. Acta* **2012**, *95*, 1623−1629.
(21) Yadav, J. S.; Thrimurtulu, N.; Venkatesh, M.; Rao, K. V. R.; Prasad, A. R.; Reddy, B. V. S. *Synthesis* **2010**, 73−78.
(22) Xing, Y.; O'Doherty, G. A. *Org. Lett.* **2009**, *11*, 1107−1110.
(23) Lu, K. J.; Chen, C. H.; Hou, D. R. *Tetrahedron* **2009**, *65*, 225−231.
(24) Gerlach, H.; Oertle, K.; Thalmann, A. *Helv. Chim. Acta* **1976**, *59*, 755−760.
(25) Rao, A. V. R.; Reddy, S. P. *Synth. Commun.* **1986**, *16*, 1149−1153.
(26) Ducoux, J. P.; Lemenez, P.; Kunesch, N.; Wenkert, E. *J. Org. Chem.* **1993**, *58*, 1290−1292.
(27) Mochizuki, N.; Yamada, H.; Sugai, T.; Ohta, H. *Bioorg. Med. Chem.* **1993**, *1*, 71−75.
(28) Ballini, R.; Marcantoni, E.; Petrini, M. *Liebigs Ann. Chem.* **1995**, 1381−1383.
(29) Mahajan, J. R.; Resck, I. S. *Synth. Commun.* **1996**, *26*, 3809−3819.
(30) Banwell, M. G.; Jolliffe, K. A.; Loong, D. T. J.; McRae, K. J.; Vounatsos, F. *J. Chem. Soc., Perkin Trans. 1* **2002**, 22−25.
(31) Banwell, M. G.; Loong, D. T. J. *Org. Biomol. Chem.* **2004**, *2*, 2050−2060.
(32) Austin, K. A. B.; Banwell, M. G.; Loong, D. T. J.; Rae, A. D.; Willis, A. C. *Org. Biomol. Chem.* **2005**, *3*, 1081−1088.
(33) Banwell, M. G.; Loong, D. T. J.; Willis, A. C. *Aust. J. Chem.* **2005**, *58*, 511−516.
(34) Pandey, S. K.; Kumar, P. *Tetrahedron Lett.* **2005**, *46*, 6625−6627.
(35) Chou, C. Y.; Hou, D. R. *J. Org. Chem.* **2006**, *71*, 9887−9890.
(36) Haug, T. T.; Kirsch, S. F. *Org. Biomol. Chem.* **2010**, *8*, 991−993.
(37) Rajesh, K.; Suresh, V.; Selvam, J. J. P.; Rao, C. B.; Venkateswarlu, Y. *Synthesis* **2010**, 1381−1385.
(38) Prasad, K. R.; Gandi, V. R. *Tetrahedron: Asymmetry* **2011**, *22*, 499−505.
(39) Si, D.; Sekar, N. M.; Kaliappan, K. P. *Org. Biomol. Chem.* **2011**, *9*, 6988−6997.
(40) Prasad, K. R.; Revu, O. *Synthesis* **2012**, *44*, 2243−2248.
(41) Reddy, C. R.; Rao, N. N.; Sujitha, P.; Kumar, C. G. *Synthesis* **2012**, *44*, 1663−1666.
(42) Si, D.; Kaliappan, K. P. *Synlett* **2012**, 2822−2826.
(43) Ayyangar, N. R.; Chanda, B.; Wakharkar, R. D.; Kasar, R. A. *Synth. Commun.* **1988**, *18*, 2103−2109.
(44) Mori, K.; Sakai, T. *Liebigs Ann. Chem.* **1988**, *1988*, 13−17.
(45) Thijs, L.; Egenberger, D. M.; Zwanenburg, B. *Tetrahedron Lett.* **1989**, *30*, 2153−2156.
(46) Yadav, J. S.; Krishna, P. R.; Gurjar, M. K. *Tetrahedron* **1989**, *45*, 6263−6270.
(47) Yang, H. B.; Kuroda, H.; Miyashita, M.; Irie, H. *Chem. Pharm. Bull.* **1992**, *40*, 1616−1618.
(48) Bestmann, H. J.; Kellermann, W.; Pecher, B. *Synthesis* **1993**, 149−152.
(49) Takano, S.; Murakami, T.; Samizu, K.; Ogasawara, K. *Heterocycles* **1994**, *39*, 67−72.
(50) Kamezawa, M.; Kitamura, M.; Nagaoka, H.; Tachibana, H.; Ohtani, T.; Naoshima, Y. *Liebigs Ann. Chem.* **1996**, 167−170.
(51) Sharma, A.; Sankaranarayanan, S.; Chattopadhyay, S. *J. Org. Chem.* **1996**, *61*, 1814−1816.
(52) Kobayashi, Y.; Nakano, M.; Kumar, G. B.; Kishihara, K. *J. Org. Chem.* **1998**, *63*, 7505−7515.
(53) Dorling, E. K.; Thomas, E. J. *Tetrahedron Lett.* **1999**, *40*, 471−474.
(54) Kaisalo, L.; Koskimies, J.; Hase, T. *Synth. Commun.* **1999**, *29*, 399−407.
(55) Kalita, D.; Khan, A. T.; Barua, N. C.; Bez, G. *Tetrahedron* **1999**, *55*, 5177−5184.
(56) Doyle, M. P.; Hu, W. H.; Phillips, I. M.; Wee, A. G. H. *Org. Lett.* **2000**, *2*, 1777−1779.
(57) Ronsheim, M. D.; Zercher, C. K. *J. Org. Chem.* **2003**, *68*, 1878−1885.
(58) Tian, J.; Yamagiwa, N.; Matsunaga, S.; Shibasaki, M. *Org. Lett.* **2003**, *5*, 3021−3024.
(59) Rao, K. S.; Reddy, D. S.; Mukkanti, K.; Pal, M.; Iqbal, J. *Tetrahedron Lett.* **2006**, *47*, 6623−6626.
(60) Babu, K. V.; Sharma, G. V. M *Tetrahedron: Asymmetry* **2008**, *19*, 577−583.
(61) Sabitha, G.; Chandrashekhar, G.; Yadagiri, K.; Yadav, J. S. *Tetrahedron Lett.* **2010**, *51*, 3824−3826.
(62) Hoegenauer, E. K.; Thomas, E. J. *Org. Biomol. Chem.* **2012**, *10*, 6995−7014.
(63) Risi, R. M.; Burke, S. D. *Org. Lett.* **2012**, *14*, 1180−1182.
(64) Lu, S.; Kurán, T.; Yang, G.; Sun, P.; Mándi, A.; Krohn, K.; Draeger, S.; Schulz, B.; Yi, Y.; Li, L.; Zhang, W. *Eur. J. Org. Chem.* **2011**, *2011*, 5452−5459.
(65) Lu, S.; Sun, P.; Li, T.; Kurtán, T.; Mándi, A.; Antus, S.; Krohn, K.; Draeger, S.; Schulz, B.; Yi, Y.; Li, L.; Zhang, W. *J. Org. Chem.* **2011**, *76*, 9699−9710.
(66) Geng, W.-L.; Wang, X.-Y.; Kurtán, T.; Mándi, A.; Tang, H.; Schulz, B.; Sun, P.; Zhang, W. *J. Nat. Prod.* **2012**, *75*, 1828−1832.
(67) Singh, S. B.; Herath, K.; Guan, Z.; Zink, D. L.; Dombrowski, A. W.; Polishook, J. D.; Silverman, K. C.; Lingham, R. B.; Felock, P. J.; Hazuda, D. J. *Org. Lett.* **2002**, *4*, 1431−1434.
(68) Flack, H. D. *Acta Crystallogr.* **1983**, *A39*, 876−881.
(69) Zhang, Q.; Mándi, A.; Li, S.; Chen, Y.; Zhang, W.; Tian, X.; Zhang, H.; Li, H.; Zhang, W.; Zhang, S.; Ju, J.; Kurtán, T.; Zhang, C. *Eur. J. Org. Chem.* **2012**, *2012*, 5256−5262.
(70) Zhou, Y.; Debbab, A.; Mándi, A.; Wray, V.; Schulz, B.; Müller, W. E. G.; Kassack, M.; Lin, W.; Kurtán, T.; Proksch, P.; Aly, A. H. *Eur. J. Org. Chem.* **2013**, *2013*, 894−906.

(71) Grimme, S. *J. Comput. Chem.* **2006**, *27*, 1787−1799.
(72) Pescitelli, G.; Kurtán, T.; Krohn, K. *Comprehensive Chiroptical Spectroscopy*; Wiley: New York, 2012; Vol. 2, pp 217−249.
(73) Seco, J. M.; Quiñoá, E.; Riguera, R. *Chem. Rev.* **2004**, *104*, 17−118.
(74) Gonnella, N. C.; Nakanishi, K. *J. Am. Chem. Soc.* **1982**, *104*, 3775−3776.
(75) Greve, H.; Schupp, P. J.; Eguereva, E.; Kehraus, S.; König, G. M. *J. Nat. Prod.* **2008**, *71*, 1651−1653.
(76) Zhou, Y.; Mándi, A.; Debbab, A.; Wray, V.; Schulz, B.; Müller, W. E. G.; Lin, W.; Proksch, P.; Kurtán, T.; Aly, A. H. *Eur. J. Org. Chem.* **2011**, , 6009−6019.
(77) The dendrodolides have an 11*R* methyl group in common.
(78) Maurizis, J. C.; Pavia, A. A.; Pucci, B. *Bioorg. Med. Chem. Lett.* **1993**, *3*, 161−164.
(79) Rychnovsky, S. D.; Rogers, B. N.; Richardson, T. I. *Acc. Chem. Res.* **1998**, *31*, 9−17.
(80) Kwon, H. C.; Kauffman, C. A.; Jensen, P. R.; Fenical, W. *J. Org. Chem.* **2009**, *74*, 675−684.
(81) Rodphaya, D.; Nihira, T.; Sakuda, S.; Yamada, Y. *J. Antibiot.* **1988**, *41*, 1649−58.
(82) Cox, R. J. *Org. Biomol. Chem.* **2007**, *5*, 2010−2026.
(83) Chooi, Y. H.; Tang, Y. *J. Org. Chem.* **2012**, *77*, 9933−9953.
(84) Zhou, H.; Gao, Z.; Qiao, K.; Wang, J.; Vederas, J. C.; Tang, Y. *Nat. Chem. Biol.* **2012**, *8*, 331−333.
(85) Pescitelli, G.; Kurtán, T.; Flörke, U.; Krohn, K. *Chirality* **2009**, *21*, E181−E201.
(86) Mosmann, T. *J. Immunol. Methods* **1983**, *65*, 55−63.
(87) Frisch, M. J.; Trucks, G. W.; Schlegel, H. B.; Scuseria, G. E.; Robb, M. A.; Cheeseman, J. R.; Scalmani, G.; Barone, V.; Mennucci, B.; Petersson, G. A.; Nakatsuji, H.; Caricato, M.; Li, X.; Hratchian, H. P.; Izmaylov, A. F.; Bloino, J.; Zheng, G.; Sonnenberg, J. L.; Hada, M.; Ehara, M.; Toyota, K.; Fukuda, R.; Hasegawa, J.; Ishida, M.; Nakajima, T.; Honda, Y.; Kitao, O.; Nakai, H.; Vreven, T.; Montgomery, J. A., Jr.; Peralta, J. E.; Ogliaro, F.; Bearpark, M.; Heyd, J. J.; Brothers, E.; Kudin, K. N.; Staroverov, V. N.; Kobayashi, R.; Normand, J.; Raghavachari, K.; Rendell, A.; Burant, J. C.; Iyengar, S. S.; Tomasi, J.; Cossi, M.; Rega, N.; Millam, J. M.; Klene, M.; Knox, J. E.; Cross, J. B.; Bakken, V.; Adamo, C.; Jaramillo, J.; Gomperts, R.; Stratmann, R. E.; Yazyev, O.; Austin, A. J.; Cammi, R.; Pomelli, C.; Ochterski, J. W.; Martin, R. L.; Morokuma, K.; Zakrzewski, V. G.; Voth, G. A.; Salvador, P.; Dannenberg, J. J.; Dapprich, S.; Daniels, A. D.; Farkas, O.; Foresman, J. B.; Ortiz, J. V.; Cioslowski, J.; Fox, D. J. *Gaussian 09, Revision B.01*, Gaussian, Inc., Wallingford, CT, 2010.
(88) Stephens, P. J.; Harada, N. *Chirality* **2010**, *22*, 229−233.
(89) *MacroModel*; Schrödinger LLC, 2012; http://www.schrodinger.com/productpage/14/11/.
(90) Varetto, U. *MOLEKEL 5.4*; Swiss National Supercomputing Centre, Manno, Switzerland, 2009.